ROYAL SOCIETY
OF CHEMISTRY

www.rsc.org/crystengcomm

Synthetic Strategies for New Vanadium Oxyfluorides Containing Novel Building Blocks: Structures of V(IV) and V(V) Containing $Sr_4V_3O_5F_{13}$, $Pb_7V_4O_8F_{18}$, $Pb_2VO_2F_5$, and Pb_2VOF_6

Jeongho Yeon,[1] Justin B. Felder,[1] Mark D. Smith,[1] Gregory Morrison,[1] and Hans-Conrad zur Loye,[1*]

[1]Department of Chemistry and Biochemistry, University of South Carolina, Columbia, SC 29208

Abstract

Four new vanadium oxyfluorides (VOFs), $Sr_4V_3O_5F_{13}$ (**1**), $Pb_7V_4O_8F_{18}$ (**2**), $Pb_2VO_2F_5$ (**3**), and Pb_2VOF_6 (**4**), have been synthesized under mild hydrothermal conditions. The choice of starting reagents, AF_2 or $A(CH_3CO_2)_2 \cdot xH_2O$ (A = Pb, Alkaline Earth), determined the oxidation states of vanadium in the final products. The reaction of V_2O_5 with AF_2 leads, consistently, to the formation of V(V) compounds, while the use of $A(CH_3CO_2)_2 \cdot xH_2O$ results in V(IV) containing compounds, suggesting that the acetate species behaves as an effective mild reducing agent. The crystal structures, characterized by single crystal X-ray diffraction, revealed that the compounds exhibit various anionic VOF building blocks, including dimeric and trinuclear units, as well as one-dimensional chains. All compounds contain fluorine atoms that are not bonded to the vanadium atoms, which are located between two-dimensional layers consisting of corner- or edge-shared FA_3 or FA_4 polyhedra that separate the vanadium containing building blocks. The magnetic susceptibility data for **4** were measured as a function of temperature, yielding an effective magnetic moment of 1.72 μ_B that confirms the presence of V(IV). UV-vis reflectance and thermal properties were also characterized.

Introduction

Materials discovery via the assembly of novel building blocks (BBs) continues to be a rewarding pursuit, especially when the new BBs favor the formation of previously unexplored compositions and/or unique structure types. Oxyfluoride groups, $M_xO_yF_z$, represent one class of potentially unique BBs, as they contain two very different bonding environments arising from the simultaneous presence of metal-oxide (M–O) and metal-fluoride (M–F) bonds. Although oxygen and fluorine atoms are both considered highly electronegative elements, when bonded to transition metals they differ significantly in their bond ionicities,[1] which impacts the observed physical properties. In other words, electronic and magnetic interactions are likely influenced by the relatively more covalent M–O bonds, whereas optical properties are influenced by the optical transparency created by the large band gaps commonly observed for the more ionic M–F bonds. Furthermore, from a structural standpoint, the fluorine atom can effectively substitute for the oxygen atom in the metal coordination environment resulting in diverse bonding motifs, which directly impacts the oxidation state of the metal ion and promotes new compositions and diverse structure types. These effects are clearly observed in the title compounds, where the replacement of one oxygen atom by a fluorine atom in the vanadium coordination sphere results in a unique structural stacking motif of the BBs, as well as in the stabilization of magnetic V(IV) in some of the crystal structures.

We are particularly interested in vanadium oxyfluorides (VOFs) because the vanadium exhibits a rich structural chemistry stemming from its various coordination environments that include tetrahedral, square planar, and octahedral, and from the ability of vanadium to take on oxidation states ranging from +2 to +5.[2-7] Thus, the formation of diverse VOFs with new BBs can be expected to promote unprecedented crystal structures giving rise to interesting physical

3

properties. For example, when the VOFs contain reduced vanadium species, low dimensional magnetism can potentially be observed.[8-10] Also, highly asymmetric local coordination spheres that are inevitably created by the presence of two distinct bonding motifs around the vanadium center, will frequently result in nonlinear optical behavior, such as a second-harmonic generation, when the crystal structure is non-centrosymmetric.[11-14]

A significant number of VOFs have been reported; however, the majorities of those are compounds containing monovalent (alkali or ammonium) cations[10, 12, 15-39] or are organically templated hybrid materials.[5, 40-49] To the best of our knowledge only a very small number of purely inorganic VOFs containing divalent (alkaline earth or lead) cations have been reported in the literature, including $Sr_5F(VOF_5)_3(H_2O)_3$,[17] $BaVOF_4$,[22] $Ba_3V_2O_4F_8$,[23] $PbVOF_5$,[16] $PbV_2O_2F_8$,[16] and $Pb_3F(V_4O_3F_{18})$.[16] This dearth of compositions prompted us to explore new A^{2+}–VOFs systems in order to develop novel structural BBs and, with them, to expand the crystal chemistry of VOFs. We utilized a mild hydrothermal approach that we have developed as an effective approach to create VOFs, and successfully synthesized several new compositions containing either fully oxidized V(V) or slightly reduced V(IV) in the crystal structures. For the preparation of materials containing V(IV), which is generally considered a relatively rare oxidation state of vanadium when compared to the ubiquitousness of V(III) or V(V) containing structures, synthetic routes based on either the preservation of the V(IV) oxidation state present in a reagent or the in-situ reduction of V(V), are effective. In both cases, however, it is challenging to preserve the V(IV) species due to the tendency of V(IV) to disproportionate into V(III) and V(V).

We previously reported on a convenient two-step hydrothermal method that involved the in-situ creation of V(IV) using oxalic or tartaric acid as the reducing agent.[50, 51] In this approach, a relatively slow cation reduction process occurs in step one, followed by the formation of crystals

of V(IV) containing products in step two. However, under these reaction conditions it is difficult

to avoid the incorporation of excess organic oxalate or tartrate groups into the product structure,

since these ligands readily chelate the vanadium centers and create organic-inorganic hybrid

materials rather than pure inorganic VOFs. More recently, we found that the acetate group can

also function as an effective mild reducing agent under acidic reaction conditions and resists

incorporation into the crystalline product. Thus, utilizing acetate as a reducing agent, we

succeeded in preparing a host of new pure inorganic fluoride compounds.[52-55] As described in

this paper, by adapting this method toward the synthesis of new VOFs we were able selectively

to grow single crystals of either V(IV) or V(V) containing VOFs. Herein, the synthesis, crystal

structures, and magnetic properties of four new VOFs are discussed.

Experimental Section

Reagents

V_2O_5 (Alfa Aesar, 99.6%), SrF_2 (Alfa Aesar, 99%), BaF_2 (Alfa Aesar, 99%), PbF_2 (Alfa Aesar,

99%), MnF_2 (Alfa Aesar, 99%), CoF_2 (Alfa Aesar, 98%), $Sr(CH_3CO_2)_2$ (Reagent Grade),

$Ba(CH_3CO_2)_2$ (ACS Grade), $Pb(CH_3CO_2)_2 \cdot 3H_2O$, and HF (Alfa Aesar, 48%) were used as

received. *Caution: Hydrofluoric acid is toxic and corrosive, must be handled with extreme care,*

and appropriate protective gear must be worn! If contact with the liquid or vapor occurs, proper

treatment procedures should immediately be implemented.[56-58]

Synthesis

Single crystals of the reported oxyfluorides were obtained via a mild hydrothermal route. For

typical reactions, 1 mmol of AF_2 or $Pb(CH_3CO_2)_2 \cdot xH_2O$, 2 mmol of V_2O_5 (0.5 mmol for **4**) were

combined with 1 mL of HF and 1 mL of H_2O. For the synthesis of **3**, 1 mmol of MnF_2 or CoF_2

was additionally added to the mixture. The respective solutions were then placed into 23 mL Teflon–lined autoclaves. The autoclaves were closed, heated to 200 °C at a rate of 5 °C m^{-1}, held for 1 day, and cooled to room temperature at a rate of 6 °C h^{-1}. The mother liquor was decanted from the single crystal products, which were isolated by filtration and washed with distilled water and acetone. In all cases, the reaction yielded a single phase product in approximately 70 % yield based on V_2O_5.

Single Crystal X–ray Diffraction

X-ray intensity datasets from yellow or blue crystals were collected at 100(2) K using a Bruker SMART APEX diffractometer or a Bruker D8 QUEST diffractometer equipped with a PHOTON 100 CMOS area detector and an Incoatec microfocus source (Mo Kα radiation, 0.71073 Å).[59] The raw area detector data frames were reduced and corrected for absorption effects with the SAINT+ and SADABS programs.[59] Final unit cell parameters were determined by least-squares refinement of a large number of reflections taken from the data set. Direct methods structure solution, difference Fourier calculations and full-matrix least-squares refinement against F^2 were performed with SHELXL-2014 using the ShelXle interface.[60, 61]

The respective space groups were confirmed by obtaining sensible and stable refinements for the structures. It should be noted that compound **1** contains some disordered atomic sites, specifically the mixed oxide/fluoride site O(7)/F(7), which was assigned for charge balance reasons. One such site is necessary to generate the reported electroneutral crystal composition, assuming V^{+5}. This site was identified as follows: The two oxygen atoms O(1) and O(2) were unambiguously assigned on the basis of bond distances (V(1)-O = 1.600 and 1.724 Å), displacement parameter behavior and trial refinements of the site occupancy factors (*sof*s). *Sof*s of the remaining anion sites F1-F7 were refined, beginning with fluorine scattering factors. Sites

F(1)-F(6) remained at 100% fluorine within experimental error, while the "F(7)" *sof* decreased to 0.89(1). This was accompanied by a *ca*. 0.1% drop in the *R* value and a normalization of the inflated "F(7)" displacement parameter. Conversely, if refined as oxygen, the "O(7)" *sof* grew to 1.07(1). This site was subsequently refined as a 50% O / 50% F site with common positional and anisotropic displacement parameters; no evidence for a partially ordered O/F split site was observed from the difference map. Exact 50/50 disorder of vanadium V(2) is imposed by the inversion center in the space group $P2_1/n$. Trial refinements in subgroups $P2_1$ and Pn, which lack inversion symmetry, were undertaken. Solutions in both groups showed two independent disordered V(2) sites with occupancies refining to near 50% each. $P2_1/n$ was therefore retained as the correct group. Additionally, efforts to observe ordering of the O/F site in these lower symmetry groups gave further support for the O7/F7 mixed site model. In $P2_1$ and Pn, there are two symmetry-independent "O7/F7" sites corresponding to the two equivalent inversion-related sites in $P2_1/n$. Both independent sites still refine best as mixed O/F positions in the lower groups, with an ordered O and F model giving physically unrealistic displacement parameters. For the above reasons, this compound is best understood as a disordered crystal with $P2_1/n$ space group symmetry, a split vanadium position and a scrambled O/F axial site around the inversion-related vanadium centers. All atoms were refined with anisotropic displacement parameters. No deviation from full occupancy was observed for Sr(1), Sr(2) or V(1). Crystallographic data and selected interatomic distances are listed in Tables 1 and 2, respectively.

Powder X–ray Diffraction

Powder X-ray diffraction data were collected on a Rigaku D/Max-2100 powder X-ray diffractometer using Cu Kα radiation. The step-scan covered the angular range 5-70° 2θ in steps

of 0.02°. No impurities were observed, and the calculated and experimental PXRD patterns on ground crystals are in excellent agreement.

UV–vis Diffuse Reflectance Spectroscopy

Diffuse reflectance spectra of polycrystalline powder samples of the reported materials were obtained using a Perkin Elmer Lambda 35 UV/vis scanning spectrophotometer equipped with an integrating sphere in the range 200 – 900 nm.

Energy Dispersive Spectroscopy

Elemental analysis was performed on single crystals of the reported series using a Thermo EDS equipped Tescan Vega-3 SEM utilized in the low vacuum mode. The crystals were mounted on carbon tape and analyzed using a 30 kV accelerating voltage and an accumulation time of 20 s. As a qualitative measure, Energy dispersive spectroscopy (EDS) verified the presence of the strontium, lead, oxygen, and fluorine in the reported compounds.

Magnetic Property Measurements

The magnetic properties of **4** were measured using a Quantum Design Magnetic Property Measurement System (QD-MPMS3 SQUID VSM). Temperature dependent susceptibility measurements were performed in both zero-field cooled (zfc) and field cooled (fc) conditions in applied fields of 1000 Oe. Magnetization measurements at 2 K were carried out in applied field up to 5 T. Corrections for the radial offset and sample shape were applied to the magnetic data using a fitting routine that involved data collected at 30 K under both DC and VSM scan modes.[62]

Results

Synthesis

The purpose of our investigation was to explore unique synthetic methods to create novel compounds containing anionic $V_xO_yF_z$ building blocks while simultaneously taking advantage of synthetic conditions that provide us with control over the oxidation state of vanadium in the product. All of the title compounds, **1-4**, were synthesized via a relatively mild hydrothermal route in which the starting reagents, AF_2 or $A(CH_3CO_2)_2 \cdot xH_2O$ (A = Sr, Ba or Pb) and V_2O_5, were reacted in a dilute aqueous hydrofluoric acid environment. V(V) compounds were obtained when the divalent cation was introduced in the form of AF_2, while reduced, V(IV) containing products were obtained when the divalent cation was introduced as an acetate, indicating that the acetate group behaved as a reducing agent. It is noteworthy that in order to synthesize **3**, it was necessary to add MF_2 (M = Mn or Co) to the reaction mixture. In the absence of MF_2 (M = Mn or Co), compound **2** was the exclusive product. The role of the transition metal fluoride is not certain, however, it is likely that the metal fluoride acts as a mineralizer and promotes the formation of **3**. The oxidation states of vanadium in the final products were visually distinguishable due to their unique colors, blue and yellow/gold for V(IV) and V(V), respectively (see Fig. 1). All reactions produced high quality single crystals in excellent yield as the sole products. The purity of all samples was confirmed by powder X-ray diffraction, illustrated in Fig. S1 – S4.

Crystal structures

$Sr_4V_3O_5F_{13}$ (or $Sr_4F_2(V_3O_5F_{11})$) (**1**) crystallizes in the monoclinic space group $P2_1/n$, and consists of two independent strontium, two vanadium, six fluorine, and two oxygen atoms, as well as of one mixed O/F site in the asymmetric unit. All atoms are located on general crystallographic positions (site 4e). Vanadium atom V(2) is disordered across an inversion center (site 2c) and was refined with 50 % occupancy. As seen in Figure 2(a), all V(V) atoms are

located in highly distorted octahedra due to the presence of two distinct V-O and V-F bonding

motifs with V-O/F distances of 1.600(2) − 2.263(2) Å. In the $V(1)O_2F_4$ polyhedra, two O atoms

occupy cis positions around the V(1) atom with shorter bond distances than found for the four V-

F bonds, causing V(1) to shift towards the edge consisting of the two oxygens. The V(2) atom,

disordered over two sites with a V-V separation of 0.649(2) Å, is coordinated to two O, two F,

and two mixed O/F atoms, creating a $V(2)O_3F_3$ octahedron where the two ordered trans O atoms

bridge the adjacent V(1) and V(2) atoms. The distances between V and terminal O atoms

(hereafter referred as Ot) are shorter than the others due to their 'vanadyl', V=O, character. Also,

the V-F bonds that are trans to the short V-O bonds are correspondingly longer, due to the trans

effect that elongates the V-F axial bond opposite the very short vanadyl bond.

The most interesting structural feature of **1** is the presence of this new trinuclear $V_3O_5F_{11}$

building block, which is composed of corner-shared $V(1)O_2F_4$ and $V(2)O_3F_3$ polyhedra that

exclusively connect via O atoms. The $V_3O_5F_{11}$ BBs are separated from each other by Sr and F(1)

atoms. To emphasize the connectivity in the structure, the composition is best written as

$[2(V(1)O_{1/2}O_{1/1}F_{4/1})]^{4-}[V(2)O_{2/2}O_{1/1}F_{3/1}]^{2-}$ with charge balance provided by an $Sr_4F_2^{6+}$ unit. The

$V_3O_5F_{11}$ BBs are stacked along the *c* axis, rotating 90° every *c*/2 to orient along the [-1 1 0] and

[1 1 0] directions (see Fig. 3). The Sr atoms exhibit 9- and 10-fold coordination spheres, resulting

in irregular SrO_xF_y polyhedra with Sr-O/F distances of 2.447(2) − 2.743(2) Å.

$Pb_7V_4O_8F_{18}$ (or $Pb_7F_6(V_4O_8F_{12})$) (**2**) crystallizes in the monoclinic space group $P2_1/n$, and there

are 19 atomic positions in the asymmetric unit: four independent lead, two vanadium, four

oxygen, and nine fluorine atoms. All atoms are located on general positions (site 4*e*), except for

Pb(4), which is located on an inversion center (site 2*a*). Compound **2** exhibits a new building

block, the 1-D zigzag-like $V_4O_8F_{12}$ chain shown in Fig. 2(b) and 4, which consists of $V(1)O_3F_3$

and V(2)O$_2$F$_4$ polyhedra that corner share via the O(3) and F(2) atoms. All V atoms are located in heavily distorted octahedra with V-O/F distances of 1.645(5) – 2.133(4) Å, in which V-Ot bonds are again the shortest, as expected for vanadyl groups. The trans effect in the V(1)O$_3$F$_3$ polyhedron is weakened due to the presence of two Ot atoms with similar V-O lengths, whereas in the V(2)O$_2$F$_4$ polyhedron a more obvious trans effect is observed since only one Ot atom is bonded to the V(2) atom. To emphasize the connectivity in compound **2**, the composition is best written as $[2(V(1)O_{1/2}O_{2/1}F_{1/2}F_{2/1})]^{5-}[2(V(2)O_{1/2}O_{1/1}F_{1/2}F_{3/1})]^{3-}$, with charge balance compensated by Pb$_7$F$_6{}^{8+}$ units. There are four unique Pb atoms that are observed in irregular 7- to 10-coordinated polyhedra of Pb(1)O$_2$F$_9$, Pb(2)O$_3$F$_4$, Pb(3)O$_2$F$_6$, and Pb(4)F$_{10}$ with Pb-O/F distances between 2.319(4) Å and 2.998(6) Å, all of which are further linked to the 1-D chains via O and F atoms.

Pb$_2$VO$_2$F$_5$ (or Pb$_2$F$_2$(VO$_2$F$_3$)) (**3**) crystallizes in the triclinic space group *P*-1, and the asymmetric unit consists of two lead, one vanadium, five fluorine and two oxygen atoms, all of which are located on positions of general crystallographic symmetry (2*i*). The V atom in the distorted VO$_2$F$_4$ octahedron is shifted toward the edge comprised of the two oxygens due to the shorter lengths of the V-O bonds (1.663(6) – 1.710(5) Å) compared to the longer lengths of the four V-F bonds (1.884(5) – 2.214(5) Å). Although two Ot atoms are cis positioned around the V center, the V-O(2) bond displays more vanadyl character as indicated by its shorter length compared to the V-O(1) bond. The distorted VO$_2$F$_4$ polyhedra are linked to each other through two F(5) atoms, creating V$_2$O$_4$F$_6$ dimeric BBs that are separated by Pb and F(1) and F(2) atoms (see Fig. 2(c) and 5). In terms of connectivity, doubling the formula to emphasize the anionic dimer, allows compound **3** to be written as $[2(VO_{2/1}F_{2/1}F_{2/2})]^{4-}$, with charge balance maintained by

$Pb_4F_4^{4+}$ units. The two Pb atoms are found in irregular $Pb(1)O_2F_6$ and $Pb(2)O_2F_9$ polyhedra with Pb-O/F distances of 2.313(4) – 2.904(6) Å.

Pb_2VOF_6 (or $Pb_2F_2(VOF_4)$) (**4**) crystallizes in the monoclinic space group $C2/c$, and there are 11 atomic positions in the asymmetric unit: two lead, one vanadium, seven fluorine, and one oxygen atom. All atoms are on general positions (site 8f), except for fluorine atoms F(6) and F(7), which are located on two-fold axes of rotation (site 4e). The local octahedral environment around the V atom is severely distorted, such that the V center in the VOF_5 polyhedron has shifted towards one vertex, an Ot atom with a very short V-O bond (1.619(4) Å). There are four intermediate V-F lengths (1.890(4) – 1.957(4) Å) and one long V-F distance (2.238(4) A), the latter of which results from the trans effect since the F atom is located opposite to the short V-O bond. The VOF_5 polyhedra share their edges via two F(4) atoms, creating $V_2O_2F_8$ dimeric building blocks that are separated by Pb and F(5), F(6), F(7) atoms (see Fig. 2(d) and 6). To emphasize its connectivity, compound **4** can be written as $[2(VO_{1/1}F_{3/1}F_{2/2}]^{4-}$, with charge balance provided by $Pb_4F_4^{4+}$ units. The Pb(1) atom is coordinated to one O and six F atoms with Pb-O/F distances of 2.356(4) – 2.679(3) Å, while the Pb(2) atom is bonded to exclusively nine F atoms with Pb-F distances of 2.313(4) – 2.904(6) Å.

For compounds **1 – 4**, bond valence sum calculations[63, 64] resulted in values of 1.73 – 2.12, 4.02, and 4.55 – 4.92 for A^{2+}, V^{4+}, and V^{5+}, respectively.

UV-vis Diffuse Reflectance Data and Thermal Behavior

Ground crystals of the title compounds were used to collect UV-vis diffuse reflectance data that were further converted to absorbance using the Kubelka-Munk function[65] (see Fig. S5). All compounds exhibit similar spectra and absorb light across the visible region. For compound **4**, a broad absorption peak is also observed at around 650 nm, which is likely due to the d-d transition

of the V(VI) d^1 centers present in **4**. The band gaps estimated by the onset of the absorption edges yielded values of approximately 2.3 – 2.8 eV, implying semiconducting nature of the compounds.

To see if the compounds could be converted to single phase oxide materials they were all heated to 600 ˚C in air. In all cases, however, the PXRD patterns obtained for the products of the heating procedure revealed that in all cases mixtures of several oxide phases, including $Sr_2V_2O_7$,[66] $Sr_3V_2O_8$,[67] $Pb_4V_2O_9$,[68] $Pb_3V_2O_8$,[69] and at least one unidentified phase, were obtained rather than one single phase product.

Magnetic Properties

The temperature dependence of the magnetic susceptibilities for **4** was measured in an applied field of 1000 Oe, and is shown in Fig. 7. No difference between the zero-field cooled (zfc) and field cooled (fc) data was found. Also, no evidence of a magnetic transition was observed. Using a modified C-W law with a temperature independent paramagnetic term (χ_{TIP}), an effective magnetic moment of 1.72 μ_B per V(IV) was obtained, which is in excellent agreement with the expected spin only value of 1.73 μ_B for V(IV), confirming the presence of the V(IV).

Discussion

Synthetic Consideration

Table 3 provides a summary of the synthetic conditions for known, structurally characterized inorganic VOFs containing alkali or alkali earth metals, or ammonium, and includes the synthetic methods that were used to prepare these compounds. Prior to 1990, the primary approach used to prepare VOFs consisted of slow cooling or of evaporating vanadium and alkali, alkaline earth or ammonium containing HF solutions at or below room temperature. More recently, the mild hydrothermal method has been favored as a convenient technique to obtain high quality single

crystals of VOFs. Similarly, crystals of the VOFs reported in this paper were obtained via the mild hydrothermal route.

The hydrothermal method is rather general and its success often hinges on the precursor used. For example, a number of vanadium reagents, including V_2O_5, VO_2, V_2O_3, VF_3, VOF_3, and VOF_2 containing vanadium in various oxidation states, can be used and are expected to result in products potentially containing vanadium in different oxidation states. For example, V(V) compounds are expected to result from the use of V_2O_5 or VOF_3, because the reactants already contain the fully oxidized V(V). For the synthesis of V(IV) containing compounds, on the other hand, two general methodologies, one based on the preservation of the V(IV) oxidation state of the precursor, such as VO_2, and one based on the in-situ reduction of a V(V) precursor to a V(IV) solution species, are often used. In the first approach, V(IV) containing solutions are formed by dissolving V(IV) precursors, as well as other reactants, in HF(aq), heating the reaction mixtures to 200°C followed by slow cooling to grow single crystals. A related method exemplified by the second approach, relies on an in-situ reduction step of V(V) to V(IV) via the use of a mild reducing agent, such as an organic alcohol or acid; a strong reducing agent could cause unwanted further reduction to V(III).

One of the aims of this research was to control the oxidation state of vanadium in the product by employing different A^{2+} (A = Sr, Ba, or Pb) sources, either AF_2 or $A(CH_3CO_2)_2 \cdot xH_2O$, and reacting them with V_2O_5. Based on our prior experience, the acetate group, a mild reducing agent, readily creates V(IV) from V(V). Our experimental results supported our expectation that the nature of the starting reagents determine the oxidation state of vanadium in the final products. For example, when V_2O_5 was reacted with AF_2, only V(V) compounds were obtained including **1**, **2**, **3**, along with the known $Ba_3V_2O_4F_8$.[23] On the other hand, under the same reaction

14

conditions, the use of $A(CH_3CO_2)_2 \cdot xH_2O$ instead of AF_2 resulted primarily in V(IV) containing

compounds, including **4**, $Sr_5F(VOF_5)_3(H_2O)$,[17] and $BaVOF_4$,[22] suggesting that the acetate species

effectively reduced V(V) to V(IV), but stopped short of reducing V(V) to V(III). Although the

latter two compounds, $Sr_5F(VOF_5)_3(H_2O)$, and $BaVOF_4$, were previously reported in the

literature, it appears that they were obtained unexpectedly while attempting to prepare V(III)

containing compounds considering that they were synthesized from VF_3 or a mixture of V_2O_5

and V metal. Our method enables us to intentionally create such species and we believe that this

synthetic approach is an effective route for the further exploration of new VOFs containing

vanadium in the +4 and +5 oxidation state.

Structural Features

An analysis of the information provided in Table 3 reveals that for octahedrally coordinated

VO_xF_y polyhedra, VOF_5 is the most frequently encountered species, while VO_2F_4 or VO_4F_2

octahedra are observed in a much smaller number of cases. Of the title compounds, only

compound **4** contains the VOF_5 polyhedron, while **1**, **2**, and **3** contain VO_2F_4 polyhedra (see

Figure 2). In addition, compounds **1** and **2** also exhibit the VO_3F_3 polyhedron, a very rare

coordination environment in inorganic VOFs that, prior to this, had only been observed in the

ammonium salt, $(NH_4)VO_2F_2$.[34, 36]

The oxygen and fluorine atoms in VO_xF_y polyhedra can be crystallographically ordered or

disordered on one or more sites. When the O or F atoms are ordered, any connectivity between

the VO_xF_y polyhedra is typically achieved via a bridging F atom, resulting in V-F-V linkages.

Some exceptions are known, of course, such as $NaVO_2F_2$[21] and $Ba_3V_2O_4F_8$[23] containing VO_4F_2

and $VO_2F_2(O/F)_2$ polyhedra, respectively, that are bridged by O rather than F atoms. In **1** and **2**,

also, it is the O atoms that connect the VO_xF_y polyhedra to create the V-O-V linkages, which is

likely due to the high oxygen content (two and three out of 6) of the vanadium coordination sphere.

A number of different structural dimensionalities, primarily 0-D and 1-D, have been observed for the anionic BBs in VOFs and they are included in Table 3. The 0-D structures include isolated VO_xF_y polyhedra, dimeric and tetrameric BBs, whereas the 1-D structures include linear, zigzag, ladder-like, or even more complex chains. 2-D structures, although very rare, occur in VOF_3[19] or Bi_2VO_5F.[20] For the dimeric 0-D systems, two types of BBs have been reported thus far, namely $V_2O_2F_8$ and $V_2O_2F_7$ dimers, consisting of edge- and face-shared VOF_5 polyhedra, respectively. Compound **4** also contains the $V_2O_2F_8$ dimer formed by edge-sharing VOF_5 polyhedra, while compound **3** exhibits a different type of dimer, $V_2O_4F_6$, that consists of edge-sharing VO_2F_4 polyhedra. For the multinuclear 0-D systems, it is very interesting that **1** exhibits a novel trinuclear $V_3O_5F_{11}$ building block that is composed of corner-shared VO_2F_4 and VO_3F_3 polyhedra through exclusively O atoms. The similar trinuclear building block is observed in the anionic Sb_3F_{16} species, where, however, the SbF_6 polyhedra are corner-sharing through exclusively F atoms.[70] A unique 1-D feature is found in **2**, consisting of V atoms linked together via alternating O and F atoms in a $-V-O-V-F-V-$ fashion, creating zigzag type chains.

Although compounds **3** and **4** contain similar dimeric BBs, they crystallize in different structure types, which is likely influenced by the distinct VO_xF_y motifs, i.e., edge-sharing VO_2F_4 and VOF_5 polyhedra forming $V_2O_4F_6$ and $V_2O_2F_8$ dimers for **3** and **4**, respectively. The VOF_5 octahedron in **4** exhibits an obvious trans effect and has a very short V-O bond trans to a very long V-F bond. This distortion in the coordination spheres of the V atoms affects the coordination environment of the associated Pb atoms that separate the BBs with F atoms that are not connected to V atoms, but are bonded to Sr or Pb atoms, only. (From hereon these F atoms

are referred to as F_N). This results in a different stacking arrangement of the dimers and changes the surrounding environments of the Pb atoms, $Pb(1)O_2F_6$ and $Pb(2)O_2F_7$ in **3**, and $Pb(1)OF_6$ and $Pb(2)F_9$ in **4**, thereby creating two distinct structures. Finally, the unique structure of **4** is also affected by the fact that one O atom is substituted by one F atom, which lowers the anionic charge from $O_2F_5{}^{9-}$ found in **3** to $OF_6{}^{8-}$ found in **4**, respectively. The net charge in **4** is compensated by the reduction of V(V) to V(IV), which creates d^1 centers that are magnetic.

The four title compounds contain F_N atoms between BBs that are exclusively bound to A atoms (A = Sr or Pb), giving rise to F_NA_x polyhedra (see Fig. 8). The occurrence of such F_N atoms is not unprecedented and in fact can also be found in $Ba_3V_2O_4F_8$, $Sr_5F(VOF_5)_3(H_2O)_3$, and $Pb_3F(V_4O_3F_{18})$,[16] where the former has a 3-D network composed of corner- and edge-shared F_NBa_4 tetrahedra and the latter two include isolated F_NA_3 polyhedra. In compounds **1** – **4**, however, the F_NA_x polyhedra form 2-D sheets that separate the anionic BBs (see Fig. 9 – 12). For example, in **1** the F(1) atom is coordinated to only Sr atoms forming F_NSr_4 tetrahedra that create 2-D layers lying in the (1 0 1) planes and that separate the trinuclear BBs. The layers consists of two edge-shared F_NSr_4 tetrahedra that are further connected to each other via corner-sharing, resulting in squeezed 6-membered rings. For **2**, of the nine F atoms, F(7), F(8), and F(9) are exclusively bonded to the Pb atoms and are found in F_NPb_3 trigonal planar or F_NPb_4 tetrahedral coordination environments. The corner- or edge-shared F_NPb_x polyhedra arrange into 4-membered rings that consist of one F_NPb_3 and three F_NPb_4 polyhedra. These rings are located in 2-D sheets that stack in the (1 0 1) planes and that separate the 1-D chains of $V_4O_8F_{12}$ BBs. As discussed earlier, for **3** and **4**, different stacking patterns of the structural units are observed due to distinct O and F contents, which change the surrounding environments of the dimeric BBs. This leads to similar layered features, but the formation and packing patterns are uniquely

different. There are two and three F_N atoms in **3** and **4**, respectively, all of which are located in

F_NPb_3 trigonal planar or F_NPb_4 tetrahedra (see Fig. 8). For both compounds, the F_NPb_4 polyhedra

propagate along the *a* axis via edge-sharing, creating 1-D linear chains. These chains are then

linked together through two edge-shared F_NPb_3 polyhedra, approximately along *b* and *c*

directions, for **3** and **4**, respectively, creating 4-membered rings. The 2-D sheets in **3** are nearly

flat and are stacked along the *c* axis, whereas the 2-D layers in **4** are corrugated and are packed

along the *b* axis. The distinct layer formation is likely due to the arrangement of edge-shared

F_NPb_3 polyhedra, i.e., in **3** the polyhedra are aligned in the same direction, while in **4** the

polyhedra are almost perpendicularly staggered.

Magnetism

Compound **4** contains V(IV) d^1, s = ½ in the dimeric BBs, leading us to expect to observe

magnetic coupling between adjacent vanadium centers, which often takes the form of a spin-

dimer system. Spin dimer systems exhibit a broad maximum at low temperature due to a triplet

to a singlet spin state transition.[71] The susceptibility data for **4**, however, do not show such a

transition even at the lowest temperatures measured, 2K, and instead exhibits simple

paramagnetic behavior. Fitting the data to the Curie Weiss law and including a temperature

independent contribution, χ_{TIP}, results in a very reasonable value for the Curie constant of 0.368

emu·Kmol^{-1}, corresponding to an effective magnetic moment of 1.72 μ_B, consistent with the spin

only value of 1.73 μ_B. Also, a negligibly Weiss temperature of – 0.47 K is obtained, indicating

that the V(IV) centers are effectively isolated from each other and do not couple magnetically. It

is likely that the superexchange coupling between the V(IV) centers is suppressed due to a

combination of the ionic character of F atoms bridging the V(IV) centers and the V-F-V bond

angles.

18

Conclusions

We have successfully synthesized and structurally characterized several new VOFs containing divalent metals. Our experiments indicated that the oxidation state of vanadium in the final product was affected by the nature of the starting reagents, where the reaction of V_2O_5 with AF_2 (A = Pb, Alkaline Earth) leads, consistently, to the formation of V(V) compounds, while the use of $A(CH_3CO_2)_2 \cdot xH_2O$ results in V(IV) containing compounds, suggesting that the acetate species behaves as an effective mild reducing agent. Several new anionic VOFs units such as dimeric, trinuclear, and 1-D BBs were observed in the compounds synthesized. The BBs in these structures are separated by 2-D sheets consisting of FA_x polyhedra and are responsible for the low dimensional structural features. The magnetic property for the compound **4** containing V(IV) shows paramagnetic behavior.

Supporting Information

Electronic supplementary information (ESI) available: X–ray data in CIF format, powder XRD patterns, and UV-vis diffuse reflectance data. See DOI: XXX

Author Information

Corresponding Authors: *E-mail: zurloye@mailbox.sc.edu

Acknowledgments

References

1   D. M. Giaquinta and H.-C. zur Loye, *Chem. Mater.*, 1994, **6**, 365-372.

2   F. H. Aidoudi, P. J. Byrne, P. K. Allan, S. J. Teat, P. Lightfoot and R. E. Morris, *Dalton Trans.*, 2011, **40**, 4324-4331.

3   F. Himeur, P. K. Allan, S. J. Teat, R. J. Goff, R. E. Morris and P. Lightfoot, *Dalton Trans.*, 2010, **39**, 6018-6020.

4   P. De Burgomaster, W. Ouellette, H. Liu, C. J. O'Connor, G. T. Yee and J. Zubieta, *Inorg. Chim. Acta*, 2010, **363**, 1102-1113.

5   T. Mahenthirarajah, Y. Li and P. Lightfoot, *Inorg. Chem.*, 2008, **47**, 9097-9102.

6   D. W. Aldous, N. F. Stephens and P. Lightfoot, *Dalton Trans.*, 2007, 4207-4213.

7   D. W. Aldous, N. F. Stephens and P. Lightfoot, *Dalton Trans.*, 2007, 2271-2282.

8   H. Lu, R. Gautier, Z.-X. Li, W. Jie, Z. Liu and K. R. Poeppelmeier, *J. Solid State Chem.*, 2013, **200**, 105-109.

9   F. H. Aidoudi, D. W. Aldous, R. J. Goff, A. M. Z. Slawin, J. P. Attfield, R. E. Morris and P. Lightfoot, *Nat. Chem.*, 2011, **3**, 801-806.

10   D. W. Aldous, R. J. Goff, J. P. Attfield and P. Lightfoot, *Inorg. Chem.*, 2007, **46**, 1277-1282.

11   R. Gautier, R. Gautier, K. B. Chang and K. R. Poeppelmeier, *Inorg. Chem.*, 2015, **54**, 1712-1719.

12   M. D. Donakowski, R. Gautier, H. Lu, T. T. Tran, J. R. Cantwell, P. S. Halasyamani and K. R. Poeppelmeier, *Inorg. Chem.*, 2015, **54**, 765-772.

13   M. Holland, M. D. Donakowski, E. A. Pozzi, A. M. Rasmussen, T. T. Tran, S. E. Pease-Dodson, P. S. Halasyamani, T. Seideman, R. P. Van Duyne and K. R. Poeppelmeier, *Inorg. Chem.*, 2014, **53**, 221-228.

14   M. D. Donakowski, R. Gautier, J. Yeon, D. T. Moore, J. C. Nino, P. S. Halasyamani and K. R. Poeppelmeier, *J. Am. Chem. Soc.*, 2012, **134**, 7679-7689.

15   F. H. Aidoudi, C. Black, K. S. A. Arachchige, A. M. Z. Slawin, R. E. Morris and P. Lightfoot, *Dalton Trans.*, 2014, **43**, 568-575.

16   M. Lozinsek, E. Goreshnik and B. Zemva, *Z. Anorg. Allg. Chem.*, 2012, **638**, 2123-2128.

17   A. Le Bail, A.-M. Mercier and I. Dix, *Acta Crystallogr., Sect. E: Struct. Rep. Online*, 2009, **65**, i46-i47.

18   D. W. Aldous and P. Lightfoot, *Solid State Sci.*, 2009, **11**, 315-319.

19   J. Supel, U. Abram, A. Hagenbach and K. Seppelt, *Inorg. Chem.*, 2007, **46**, 5591-5595.

20   A. V. Akopjan, T. V. Serov, V. A. Dolgikh, E. I. Ardaschnikova and P. Lightfoot, *J. Mater. Chem.*, 2002, **12**, 1490-1494.

21   M. P. Crosnier-Lopez, H. Duroy, J. L. Fourquet and M. Abrabri, *Eur. J. Solid State Inorg. Chem.*, 1994, **31**, 957-965.

22   M. P. Crosnier-Lopez, H. Duroy and J. L. Fourquet, *Z. Anorg. Allg. Chem.*, 1994, **620**, 309-312.

23   M. P. Crosnier-Lopez, H. Duroy and J. L. Fourquet, *Z. Anorg. Allg. Chem.*, 1993, **619**, 1597-1602.

24   R. Stomberg, *Acta Chem. Scand., Ser. A*, 1986, **A40**, 325-330.

25   M. Leimkuehler and R. Mattes, *J. Solid State Chem.*, 1986, **65**, 260-264.

26   M. Schabert and G. Pausewang, *Z. Naturforsch., B: Anorg. Chem., Org. Chem.*, 1985, **40B**, 1437-1440.

27   M. Schabert, G. Pausewang and W. Massa, *Z. Anorg. Allg. Chem.*, 1983, **506**, 169-177.

28   J. Mazicek, V. K. Trunov and L. A. Aslanov, *Koord. Khim.*, 1982, **8**, 1550-1551.

29   R. Mattes and H. Foerster, *J. Less-Common Met.*, 1982, **87**, 237-247.

30   P. Bukovec and L. Golic, *Acta Crystallogr., Sect. B*, 1980, **B36**, 1925-1927.

31   K. Waltersson, *J. Solid State Chem.*, 1979, **28**, 121-131.

32   K. Waltersson, *J. Solid State Chem.*, 1979, **29**, 195-204.

33   K. Waltersson, *Cryst. Struct. Commun.*, 1978, **7**, 507-511.

34   H. Rieskamp and R. Mattes, *Z. Anorg. Allg. Chem.*, 1973, **401**, 158-164.

35   G. W. Bushnell and K. C. Moss, *Can. J. Chem.*, 1972, **50**, 3700-3705.

36   A. K. Sengupta and B. B. Bhaumik, *Z. Anorg. Allg. Chem.*, 1971, **384**, 255-259.

37   R. R. Ryan, S. H. Mastin and M. J. Reisfeld, *Acta Crystallogr., Sect. B*, 1971, **27**, 1270-1274.

38   G. Pausewang, *Z. Anorg. Allg. Chem.*, 1971, **381**, 189-197.

39   A. Carpy and J. Galy, *Bull. Soc. Fr. Mineral. Cristallogr.*, 1971, **94**, 24-29.

40   T. M. Smith, M. Tichenor, J. M. Vargas, C. J. O'Connor and J. Zubieta, *Inorg. Chim. Acta*, 2011, **378**, 250-256.

41   T. Kanatani, K. Matsumoto and R. Hagiwara, *Eur. J. Inorg. Chem.*, 2010, 1049-1055.

42   K. Adil, M. Leblanc, V. Maisonneuve and P. Lightfoot, *Dalton Trans.*, 2010, **39**, 5983-5993.

43   W. Ouellette, M. H. Yu, C. J. O'Connor and J. Zubieta, *Inorg. Chem.*, 2006, **45**, 7628-7641.

44   N. F. Stephens, M. Buck and P. Lightfoot, *J. Mater. Chem.*, 2005, **15**, 4298-4300.

45   R. C. Finn, J. Zubieta and R. C. Haushalter, *Prog. Inorg. Chem.*, 2003, **51**, 421-601.

46   M. E. Welk, A. J. Norquist, C. L. Stern and K. R. Poeppelmeier, *Inorg. Chem.*, 2000, **39**, 3946-3947.

47   D. J. Chesnut, D. Hagrman, P. J. Zapf, R. P. Hammond, R. LaDuca, R. C. Haushalter and J. Zubieta, *Coord. Chem. Rev.*, 1999, **190-192**, 737-769.

48   A. Stein, S. W. Keller and T. E. Mallouk, *Science (Washington, D. C., 1883-)*, 1993, **259**, 1558-1564.

49   H. Rieskamp and R. Mattes, *Z. Naturforsch., B: Anorg. Chem., Org. Chem.*, 1976, **31B**, 541-543.

50   A. J. Cortese, B. Wilkins, M. D. Smith, J. Yeon, G. Morrison, T. T. Tran, P. S. Halasyamani and H.-C. zur Loye, *Inorg. Chem.*, 2015, **54**, 4011-4020.

51   D. Abeysinghe, M. D. Smith, J. Yeon, G. Morrison and H.-C. zur Loye, *Cryst. Growth Des.*, 2014, **14**, 4749-4758.

52   J. Yeon, M. D. Smith, J. Tapp, A. Moller and H.-C. zur Loye, *J. Am. Chem. Soc.*, 2014, **136**, 3955-3963.

53   J. Yeon, M. D. Smith, J. Tapp, A. Moller and H.-C. zur Loye, *Inorg. Chem.*, 2014, **53**, 6289-6298.

54   J. Yeon, M. D. Smith, A. S. Sefat and H.-C. zur Loye, *Inorg. Chem.*, 2013, **52**, 2199-2207.

55   J. Yeon, M. D. Smith, A. S. Sefat, T. T. Tran, P. S. Halasyamani and H.-C. zur Loye, *Inorg. Chem.*, 2013, **52**, 8303-8305.

56   E. B. Segal, *Chem. Health Saf.*, 2000, **7**, 18.

57   D. Peters and R. Miethchen, *J. Fluorine Chem.*, 1996, **79**, 161.

58   J. C. Bertolini, *J. Emerg. Med.*, 1992, **10**, 163.

59   *SMART Version 5.631 and APEX2 Version 2014.9-0, SAINT+ Version 6.45 and 8.34A, and SADABS Version 2.10 and 2014/4, Bruker Analytical X-ray Systems, Inc., Madison, Wisconsin, USA, 2014.*

60   C. B. Hübschle, G. M. Sheldrick and B. Bittrich, *J. Appl. Cryst.*, 2011, **44**, 1281-1284.

61   G. M. Sheldrick, *Acta Cryst.*, 2008, **A64**, 112-122.

62   G. Morrison and H.-C. zur Loye, *J. Solid State Chem.*, 2015, **221**, 334-337.

63   N. E. Brese and M. O'Keeffe, *Acta Crystallogr*, 1991, **B47**, 192-197.

64   I. D. Brown and D. Altermatt, *Acta Crystallogr*, 1985, **B41**, 244-247.

65   P. Kubelka and F. Z. Munk, *Tech. Phys.*, 1931, **12**, 593.

66   J. A. Baglio and J. N. Dann, *J. Solid State Chem.*, 1972, **4**, 87-93.

67   W. Carrillo-Cabrera and H. G. von Schnering, *Z. Kristallogr.*, 1993, **205**, 271-276.

68   S. V. Krivovichev and P. C. Burns, *Can. Mineral.*, 2003, **41**, 951-958.

69   J. M. Kiat, P. Garnier and M. Pinot, *J. Solid State Chem.*, 1991, **91**, 339-349.

70   V. A. Petrov, A. Marchione and W. Marshall, *J. Fluorine Chem.*, 2008, **129**, 1011-1017.

71   R. L. Carlin, *Magnetochemistry (Springer-Verlag, Berlin, 1986).*

CrystEngComm Accepted Manuscript

Table 1 Crystallographic data for the reported compounds

compound	1	2	3	4
formula	$Sr_4V_3O_5F_{13}$	$Pb_7V_4O_8F_{18}$	$Pb_2VO_2F_5$	Pb_2VOF_6
fw	830.3	2124.09	592.32	595.32
temperature (K)	100(2)	100(2)	100(2)	100(2)
crystal system	Monoclinic	Monoclinic	Triclinic	Monoclinic
space group	$P2_1/n$	$P2_1/n$	P-1	$C2/c$
a (Å)	9.7805(7)	10.1963(7)	5.6675(5)	5.6675(4)
b (Å)	7.2405(5)	7.3172(5)	7.3492(6)	15.7931(12)
c (Å)	10.0361(7)	13.9271(10)	8.3152(7)	12.9995(9)
α (°)	90	90	101.2337(12)	90
β (°)	108.917(2)	99.057(2)	108.9953(13)	92.019(2)
γ (°)	90	90	110.6249(12)	90
V (Å^3)	672.33(8)	1026.12(12)	287.14(4)	1162.83(15)
Z	2	2	2	8
density (g/cm^3)	4.101	6.875	6.851	6.801
absorption coefficient (mm^{-1})	17.917	59.113	60.126	59.401
crystal size (mm^3)	0.15 × 0.08 × 0.02	0.10 × 0.07 × 0.05	0.10 × 0.06 × 0.05	0.10 × 0.05 × 0.04
2 theta range (°)	2.527 to 32.654	2.311 to 32.506	2.765 to 36.346	2.579 to 32.578
independent reflections	2435 [R(int) = 0.0472]	3702 [R(int) = 0.0589]	2785 [R(int) = 0.0407]	2120 [R(int) = 0.0423]
completeness to θ_{max}/%	100.00%	100.00%	99.80%	99.90%
data/restraints/parameters	2435 / 0 / 118	3702 / 0 / 170	2785 / 0 / 92	2120 / 0 / 93
GOF (F^2)	1.03	1.101	1.27	1.096
R $(F)^a$ $(I > 2(\sigma)I)$	0.0298	0.0306	0.0305	0.026
R_w $(F_o^2)^b$ $(I > 2(\sigma)I)$	0.0576	0.0678	0.0765	0.0564
largest diff. peak and hole (e$^-$/Å^3)	1.083 and -0.766	2.951 and -2.079	5.627 and -3.972	3.405 and -1.646

$R(F)^a = \Sigma||F_o| - |F_c||/\Sigma|F_o|$. $R_w(F_o^2)^b = [\Sigma w(F_o^2 - F_c^2)^2/\Sigma w(F_o^2)^2]^{1/2}$

Table 2 Selected interatomic distances (Å) for the reported compounds

1				2				3		4	
Sr(1)-F(1)	2.447(2)	V(1)-O(2)	1.600(2)	Pb(1)-F(9)	2.339(4)	Pb(4)-F(1)	2.603(4)	Pb(1)-F(1)	2.403(4)	Pb(1)-F(5)	2.356(4)
Sr(1)-F(2)	2.505(2)	V(1)-O(1)	1.724(2)	Pb(1)-F(1)	2.474(4)	Pb(4)-F(1)	2.603(4)	Pb(1)-F(1)	2.437(4)	Pb(1)-F(5)	2.406(3)
Sr(1)-F(5)	2.515(2)	V(1)-F(3)	1.887(2)	Pb(1)-F(9)	2.525(4)	Pb(4)-F(4)	2.619(5)	Pb(1)-F(2)	2.551(5)	Pb(1)-F(3)	2.474(3)
Sr(1)-F(1)	2.556(2)	V(1)-F(5)	1.904(2)	Pb(1)-F(8)	2.615(4)	Pb(4)-F(4)	2.619(5)	Pb(1)-O(2)	2.553(6)	Pb(1)-F(6)	2.526(3)
Sr(1)-F(4)	2.578(2)	V(1)-F(4)	1.970(2)	Pb(1)-F(8)	2.666(4)	Pb(4)-F(2)	2.649(4)	Pb(1)-F(4)	2.567(5)	Pb(1)-O(1)	2.574(4)
Sr(1)-F(3)	2.579(2)	V(1)-F(2)	2.227(2)	Pb(1)-F(6)	2.810(5)	Pb(4)-F(2)	2.649(4)	Pb(1)-F(2)	2.612(4)	Pb(1)-F(2)	2.651(3)
Sr(1)-(O/F)(7)	2.618(2)			Pb(1)-F(4)	2.816(4)	Pb(4)-F(7)	2.653(4)	Pb(1)-O(1)	2.649(5)	Pb(1)-F(7)	2.679(3)
Sr(1)-F(6)	2.625(2)	V(2)-(O/F)(7)	1.631(2)	Pb(1)-O(2)	2.878(5)	Pb(4)-F(7)	2.653(4)	Pb(1)-F(3)	2.662(4)		
Sr(1)-O(2)	2.695(2)	V(2)-F(6)	1.784(2)	Pb(1)-O(4)	2.998(6)	Pb(4)-F(5)	2.733(4)			Pb(2)-F(5)	2.373(3)
		V(2)-O(1)	1.937(2)	Pb(1)-F(3)	3.053(5)	Pb(4)-F(5)	2.733(4)	Pb(2)-F(1)	2.313(4)	Pb(2)-F(7)	2.435(3)
Sr(2)-F(2)	2.447(2)	V(2)-F(6)	1.956(2)			Pb(4)-F(3)	3.097(4)	Pb(2)-F(2)	2.408(5)	Pb(2)-F(1)	2.493(4)
Sr(2)-F(2)	2.489(2)	V(2)-O(1)	1.973(2)	Pb(2)-F(9)	2.319(4)	Pb(4)-F(3)	3.097(4)	Pb(2)-F(2)	2.528(4)	Pb(2)-F(6)	2.497(3)
Sr(2)-F(1)	2.490(2)	V(2)-(O/F)(7)	2.263(2)	Pb(2)-F(8)	2.394(4)			Pb(2)-F(4)	2.560(5)	Pb(2)-F(3)	2.613(4)
Sr(2)-F(4)	2.584(2)			Pb(2)-F(4)	2.461(4)	V(1)-O(1)	1.645(5)	Pb(2)-F(5)	2.728(4)	Pb(2)-F(2)	2.720(3)
Sr(2)-F(6)	2.600(2)			Pb(2)-F(7)	2.473(4)	V(1)-O(2)	1.685(5)	Pb(2)-F(3)	2.729(5)	Pb(2)-F(4)	2.783(4)
Sr(2)-F(3)	2.625(2)			Pb(2)-O(2)	2.703(5)	V(1)-F(3)	1.866(4)	Pb(2)-O(1)	2.796(6)	Pb(2)-F(4)	2.826(3)
Sr(2)-O(1)	2.626(2)			Pb(2)-O(4)	2.732(5)	V(1)-O(3)	1.972(5)	Pb(2)-F(5)	2.857(5)	Pb(2)-F(1)	2.892(4)
Sr(2)-F(5)	2.628(2)			Pb(2)-O(1)	2.756(5)	V(1)-F(2)	2.086(4)	Pb(2)-O(2)	2.904(6)		
Sr(2)-F(4)	2.670(2)					V(1)-F(1)	2.114(4)			V(1)-O(1)	1.619(4)
Sr(2)-F(1)	2.743(2)			Pb(3)-F(7)	2.416(4)			V(1)-O(2)	1.663(6)	V(1)-F(2)	1.890(4)
				Pb(3)-F(3)	2.440(4)	V(2)-O(4)	1.661(5)	V(1)-O(1)	1.710(5)	V(1)-F(1)	1.917(4)
				Pb(3)-F(8)	2.448(4)	V(2)-O(3)	1.715(5)	V(1)-F(3)	1.884(5)	V(1)-F(3)	1.949(4)
				Pb(3)-F(7)	2.540(4)	V(2)-F(6)	1.812(5)	V(1)-F(4)	1.927(5)	V(1)-F(4)	1.957(4)
				Pb(3)-F(5)	2.602(4)	V(2)-F(5)	1.948(4)	V(1)-F(5)	2.024(5)	V(1)-F(4)	2.238(4)
				Pb(3)-O(1)	2.636(5)	V(2)-F(4)	1.986(5)	V(1)-F(5)	2.214(5)		
				Pb(3)-F(1)	2.772(4)	V(2)-F(2)	2.133(4)				
				Pb(3)-O(3)	2.853(5)						
				Pb(3)-F(6)	3.089(4)						

Table 3 Structural and synthetic information for known inorganic VOFs. Note that the O/F represents disordered O and F atoms

compound	anionic VOFs dimensionality and brief structure description	V oxidation state
VOF_3	2-D layer of corner- or edge-shared VOF_5 via F	5
$NaVOF_4(H_2O)$	0-D isolated VO_2F_4 and VOF_5	5
$NaVO_2F_2$	1-D chain of corner- or edge-shared VO_4F_2 via O	5
$NaVO_{2-x}F_{2+x}$	1-D chains of corner- or edge-shared $V(1)O(O/F)_3F_2$ and $V(2)O(O/F)_3F_2$ via disordered (O/F)	4,5
Na_2VOF_5	0-D isolated VOF_5	5
NaV_2O_4F	2-D layers of corner- or edge-shared $V(O/F)_5$	4
Na_3VOF_5	0-D isolated VOF_5	4
$Na_4V_2O_2F_8$	0-D $V_2O_2F_8$ dimer of edge-shared VOF_5 via F	4
$KVOF_3$	1-D ladder of corner- or edge-shared VOF_5 via F	4
$KVOF_4$	1-D zigzag chain of corner-shared VOF_5 via F	5
K_2VOF_4	1-D zigzag chain of corner-shared $V(O/F)_2F_4$ via F	4
$K_2VO_2F_3$	1-D zigzag chain of corner-shared VO_2F_4 via F	5
$RbVOF_3$	1-D ladder of corner- or edge-shared VOF_5 via F	4
Rb_2VOF_4	1-D zigzag chain of corner-shared $V(O/F)_2F_4$ via F	4
$Rb_2VOF_4(H_2O)$	0-D isolated VO_2F_4	4
$CsVOF_3$	1-D ladder of corner- or edge-shared VOF_5 via F	4
$CsVOF_3(H_2O)_{0.5}$	1-D complex chain of corner- or edge-shared $V(1)OF_5$ and $V(2)OF_5$ via F	4
$CsVOF_4$	1-D zigzag chain of corner-shared VOF_5 via F	5
$Cs_2VOF_4(H_2O)$	0-D isolated VO_2F_4	4
$Cs_3V_2O_2F_7$	0-D $V_2O_2F_7$ dimer by face-shared VO_3F_3 via F	4
$Cs_3V_2O_4F_5$	1-D chains of face-shared $V(O/F)_6$	5
$(NH_4)VO_2F_2$	1-D zigzag chain of edge-shared $V(1)O_3F_3$ and $V(2)O_3F_3$	5
$(NH_4)_2VOF_4$	0-D isolated VOF_5	4
$(NH_4)_2VOF_4(H_2O)$	0-D isolated $VOF_4(H_2O)$	4
$(NH_4)_3VO_2F_4$	0-D isolated $V(1)(O/F)_6$ and $V(2)O_2F_4$	5
$Sr_5F(VOF_5)_3(H_2O)_3$	0-D isolated VOF_5, isolated FSr_3 units	4
$Sr_4F_2(V_3O_5F_{11})$	0-D corner-shared $V(1)O_2F_4$ and $V(2)O_3F_3$ via O	5
$BaVOF_4$	1-D chain of corner-shared VOF_5 via F	4
$Ba_3V_2O_4F_8$	0-D corner-shared $VO_2F_2(O/F)_2$ tetramer via O and F, 3-D network of FBa_4 units	5
$PbVOF_5$	0-D isolated VOF_5	5
$PbV_2O_2F_8$	0-D $V_2O_2F_8$ dimer of edge-shared VOF_5 via F	5
$Pb_2F_2(VOF_4)$	0-D $V_2O_2F_8$ dimer of edge-shared VOF_5 via F	4
$Pb_2F_2(VO_2F_3)$	0-D $V_2O_4F_6$ dimer of edge-shared VO_2F_4 via F	5
$Pb_3F(V_4O_3F_{18})$	0-D $V_4O_3F_{18}$ tetramer of corner-shared $V(1)OF_5$ and $V(2)F_6$ via F, isolated FPb_3 units	4,5
$Pb_7F_6(V_4O_8F_{12})$	1-D chain of corner-shared $V(1)O_3F_3$ and $V(2)O_2F_4$ via O and F	5
Bi_2VO_5F	2-D layer of corner-shared $V(O/F)_6$	4

Table 3 Continued

compound	brief synthetic procedure	year	ref. #
VOF_3	$V_2O_5/F_2(g)$ at 475 ˚C in a Cu tube, recrystallization using HF (aq) at -78 ˚C	2007	19
$NaVOF_4(H_2O)$	hydrothermal, $V_2O_5/NaCl/HF(aq)$ at 100 ˚C	2015	12
$NaVO_2F_2$	supercritical, $V_2O_5/NaF/BaF/H_2O/HF(aq)$ at 552 ˚C	1994	21
$NaVO_{2-x}F_{2+x}$	hydrothermal, $V_2O_5/NaCl/HF(aq)$ at 150 ˚C	2015	12
Na_2VOF_5	solution, $V_2O_5/NaF/H_2O/HF(aq)$ at 5 ˚C	1986	24
NaV_2O_4F	solid-state melt, VO_2/NaF at 720 ˚C in a sealed Au tube	1971	39
Na_3VOF_5	solution, $VO_2(aq)$ (from $V_2O_3/V_2O_5/HF(aq)$)/NaF/H_2O at 25 ˚C	1971	38
$Na_4V_2O_2F_8$	hydrothermal, $(V_2O_5/HF(aq))$ + $Et.Gly/NaNO_3$ at 100 ˚C	2009	18
$KVOF_3$	hydrothermal, $V_2O_5/HF(aq)/K_2CO_3/Et.Gly/H_2O$ at 160 ˚C	2014	15
$KVOF_4$	solution, $(V_2O_5/HF(aq))+KF$ at 25 ˚C	1973	34
K_2VOF_4	hydrothermal, $(V_2O_5/HF(aq))$ + $Et.Gly/KNO_3/H_2O$ at 100 ˚C	2009	18
$K_2VO_2F_3$	solution, $V_2O_5/KF/H_2O/HF(aq)$ at 5 ˚C	1971	37
$RbVOF_3$	hydrothermal, $(V_2O_5/HF(aq))$ + $Et.Gly/RbCl/H_2O$ at 100 ˚C	2007	10
Rb_2VOF_4	solution, $VO_2(aq)$ (from $V_2O_3/V_2O_5/HF(aq)$) + RbF at 200 ˚C	1985	26
$Rb_2VOF_4(H_2O)$	solution, $V_2O_3/V_2O_5/Rb_2CO_3/H_2O/HF(aq)$ at 5 ˚C	1983	27
$CsVOF_3$	hydrothermal, $(V_2O_5/HF(aq))$ + $Et.Gly/CsCl/H_2O$ at 100 ˚C	2007	10
$CsVOF_3(H_2O)_{0.5}$	solution, $VO_2(aq)$ (from $V_2O_3/V_2O_5/HF(aq)$)/Cs_2CO_3 at 25 ˚C	1979	31
$CsVOF_4$	solution, $V_2O_5/Cs_2CO_3/aHF$ at -30 ˚C	1972	35
$Cs_2VOF_4(H_2O)$	solution, $VO_2(aq)$ (from $V_2O_3/V_2O_5/HF(aq)$)/Cs_2CO_3 at 25 ˚C	1979	32
$Cs_3V_2O_2F_7$	solution, $VO_2(aq)$ (from $V_2O_3/V_2O_5/HF(aq)$)/CsF/H_2O at 25 ˚C	1978	33
$Cs_3V_2O_4F_5$	solution, $V_2O_5/Cs_2CO_3/aHF$ at 25 ˚C	1982	29
$(NH_4)VO_2F_2$	solution, $NH_4VO_3/HF(aq)/H_2SO_4$ at 25 ˚C	1971	36
$(NH_4)_2VOF_4$	solution, $VOF_2/NH_4F/HF(aq)$ at 25 ˚C	1980	30
$(NH_4)_2VOF_4(H_2O)$	solution, $VOF_2/NH_4F/HF(aq)$ at 25 ˚C	1982	28
$(NH_4)_3VO_2F_4$	solution, $V_2O_5/HF(aq)/NH_3$ or NH_4HF_2/NH_4VO_3 at 25 ˚C	1986	25
$Sr_5F(VOF_5)_3(H_2O)_3$	hydrothermal, $VF_3/SrF_2/H_2O/HF(aq)$ at 220 ˚C	2009	17
$Sr_4F_2(V_3O_5F_{11})$	hydrothermal, $V_2O_5/SrF_2/H_2O/HF(aq)$ at 200 ˚C	This work	
$BaVOF_4$	hydrothermal, $BaO/V_2O_5/V/HF(aq)$ at 200 ˚C	1994	22
$Ba_3V_2O_4F_8$	hydrothermal, $BaF_2/V_2O_5/H_2O/HF(aq)$ at 200 ˚C	1993	23
$PbVOF_5$	solution, $VOF_3/PbF_2/aHF$ at 25 ˚C	2012	16
$PbV_2O_2F_8$	solution, $VOF_3/PbF_2/aHF$ at 25 ˚C	2012	16
$Pb_2F_2(VOF_4)$	hydrothermal, $V_2O_5/Pb(CH_3CO_2)_2 \cdot 3H_2O/H_2O/HF(aq)$ at 200 ˚C	This work	
$Pb_2F_2(VO_2F_3)$	hydrothermal, $V_2O_5/PbF_2/CoF_2/H_2O/HF(aq)$ at 200 ˚C	This work	
$Pb_3F(V_4O_3F_{18})$	solution, $VOF_3/PbF_2/aHF$ at 25 ˚C	2012	16
$Pb_7F_6(V_4O_8F_{12})$	hydrothermal, $V_2O_5/PbF_2/H_2O/HF(aq)$ at 200 ˚C	This work	
Bi_2VO_5F	solid-state, BiF_3(or $BiOF$)/Bi_2O_3/V_2O_5 at 600 ˚C in a sealed tube	2002	20
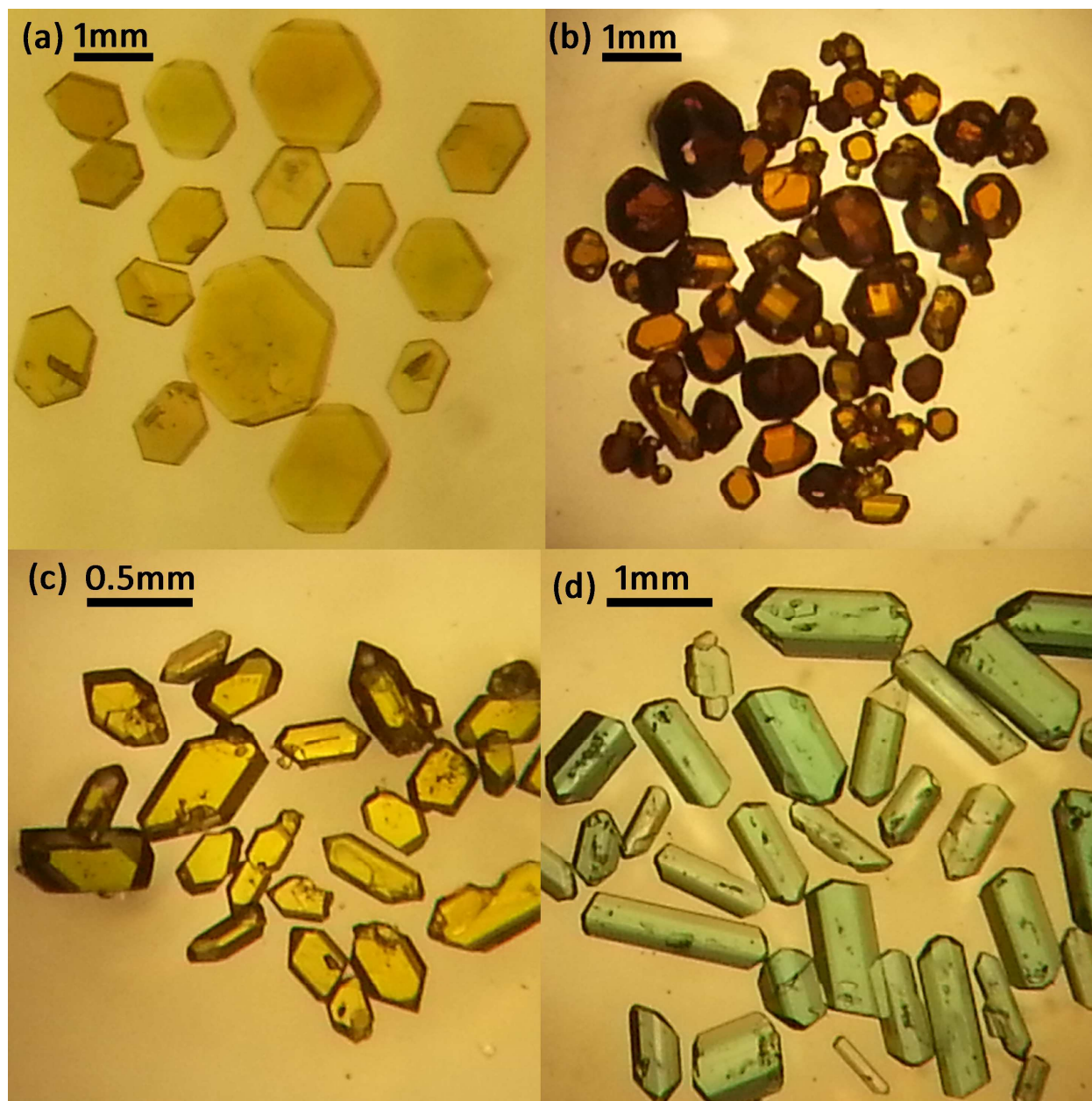
Fig. 1 Photographic images of single crystals for (a) $Sr_4V_3O_5F_{13}$, (b) $Pb_7V_4O_8F_{18}$, (c) $Pb_2VO_2F_5$, and (d) Pb_2VOF_6.
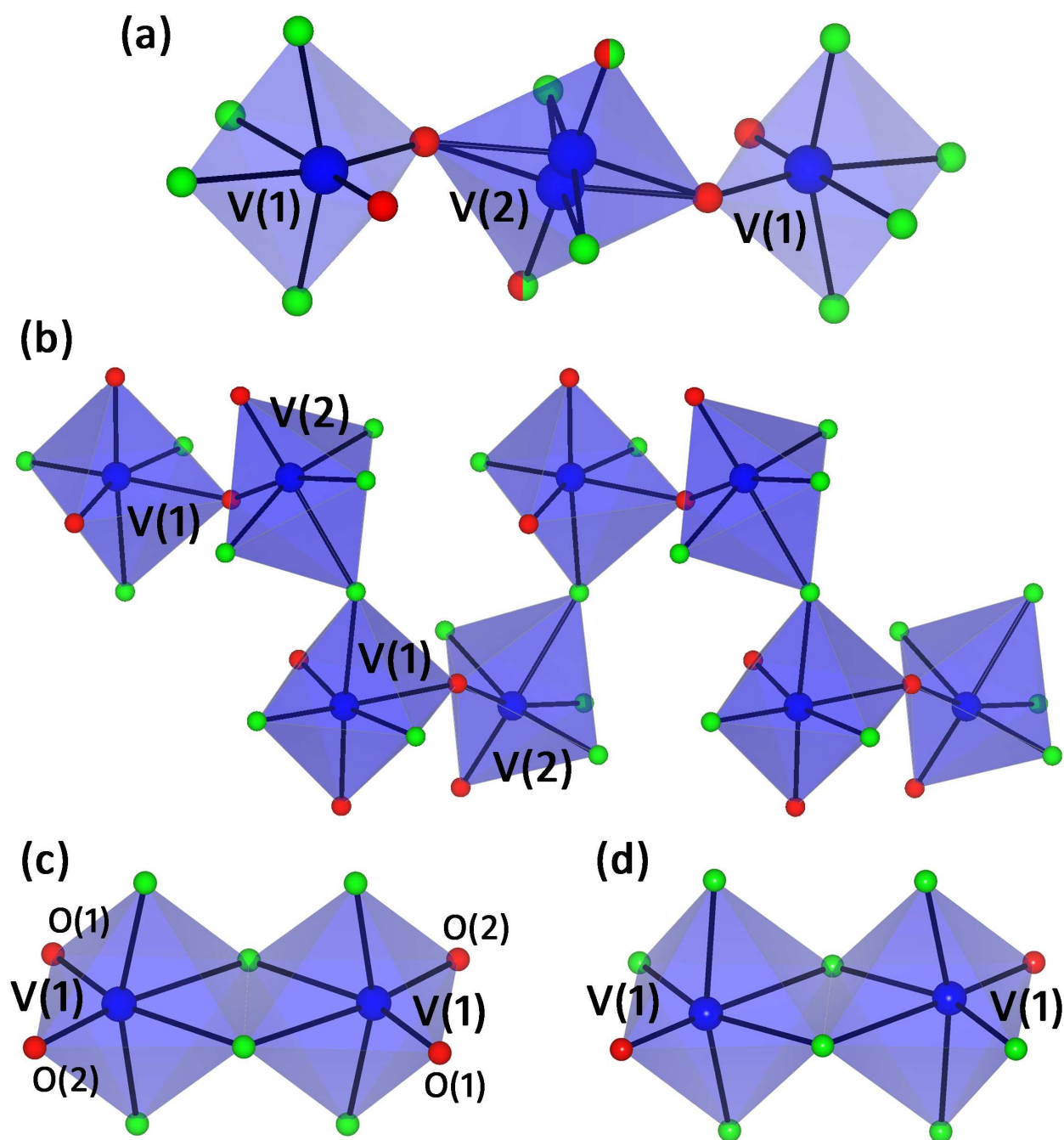
Fig. 2 Illustration of building blocks of (a) trinuclear $V_3O_5F_{11}$ in **1**, (b) $V_4O_8F_{12}$ 1-D chain in **2**, and dimeric (c) $V_2O_4F_6$ and (d) $V_2O_2F_8$ in **3** and **4**, respectively. Blue, red, and green spheres represent V, O, and F atoms.
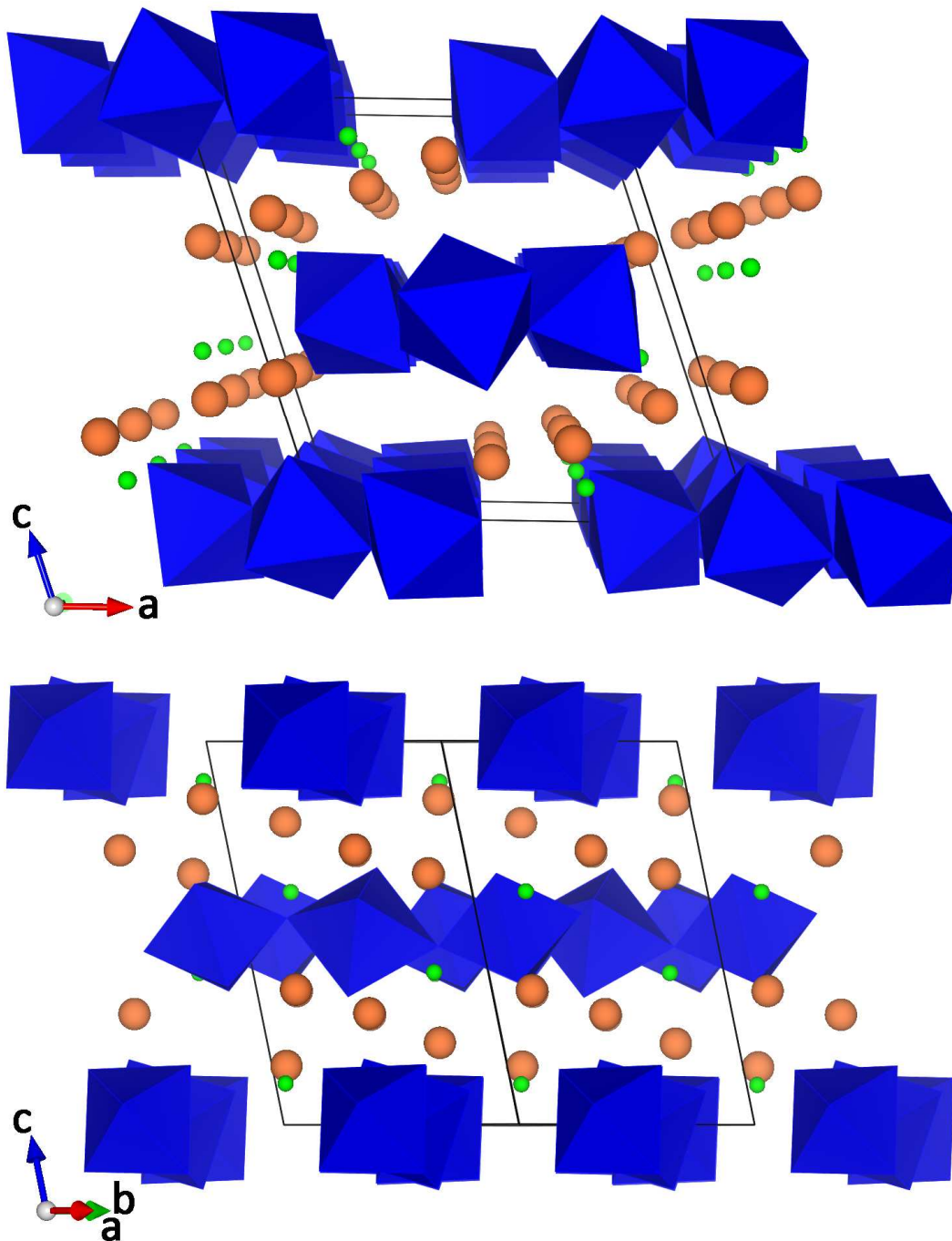
Fig. 3 Polyhedral structure representation of **1**, where the $V_3O_5F_{11}$ trinuclear building blocks are separated by Sr and F atoms. Orange, blue, and green spheres/polyhedra represent Pb, V, and F atoms/polyhedra.
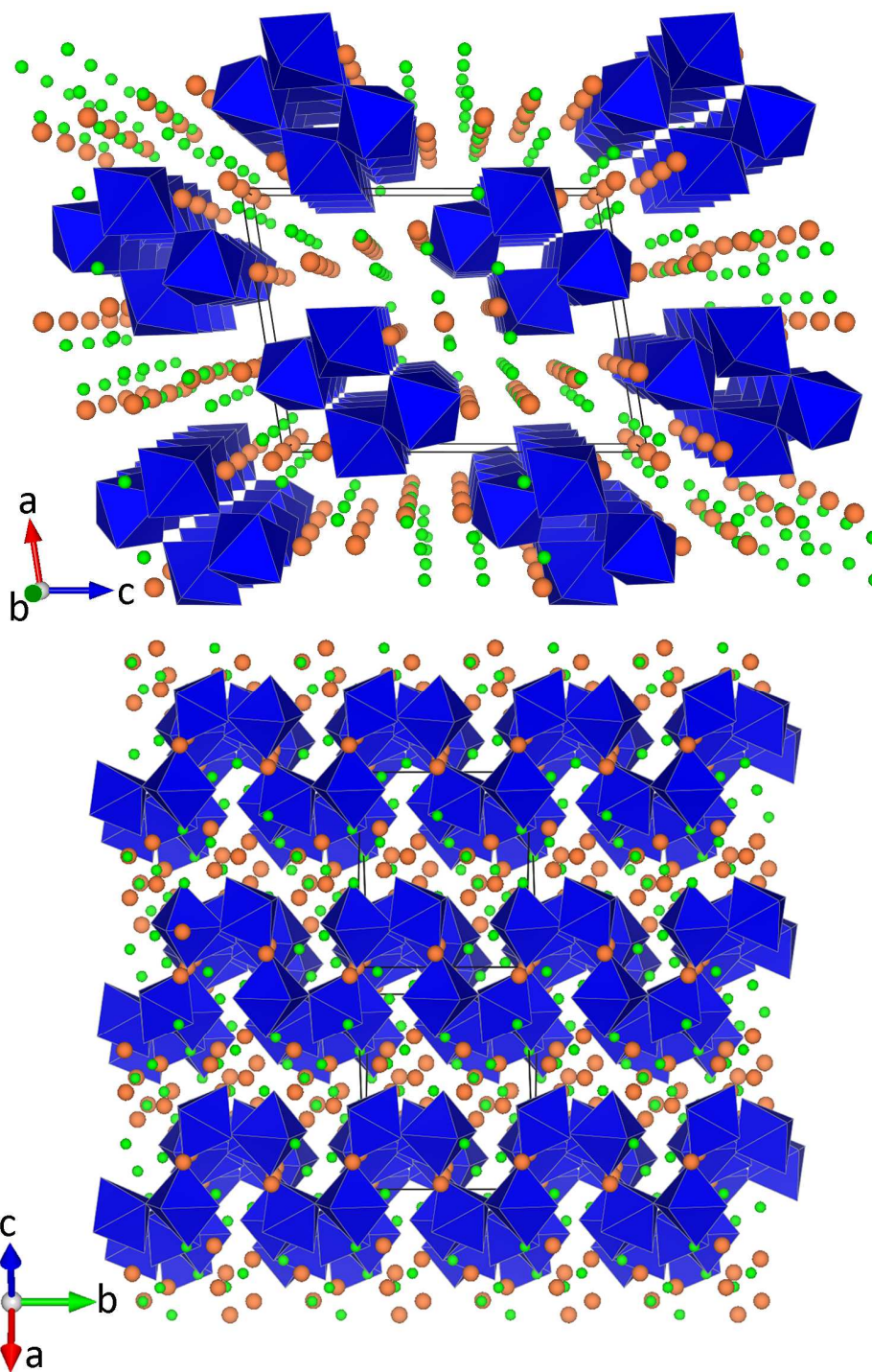
Fig. 4 Polyhedral structure representation of **2**, where the 1-D chains of $V_4O_8F_{12}$ building blocks run along the *b* axis and are disconnected by Pb and F atoms. Orange, blue, and green spheres/polyhedra represent Pb, V, and F atoms/polyhedra.
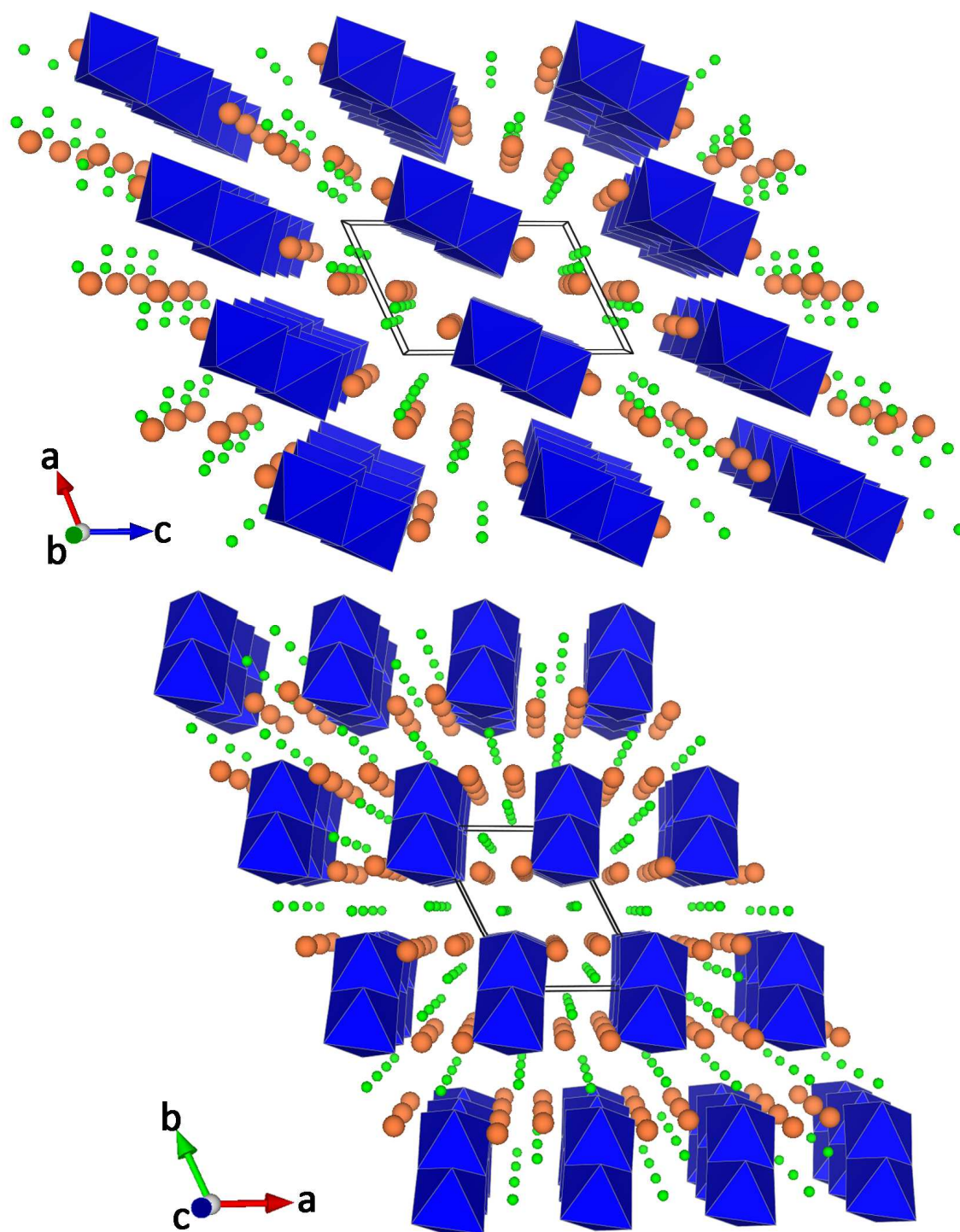
Fig. 5 Polyhedral structure representation of **3**, where the dimeric $V_2O_4F_6$ building blocks are separated by Pb and F atoms. Orange, blue, and green spheres/polyhedra represent Pb, V, and F atoms/polyhedra.
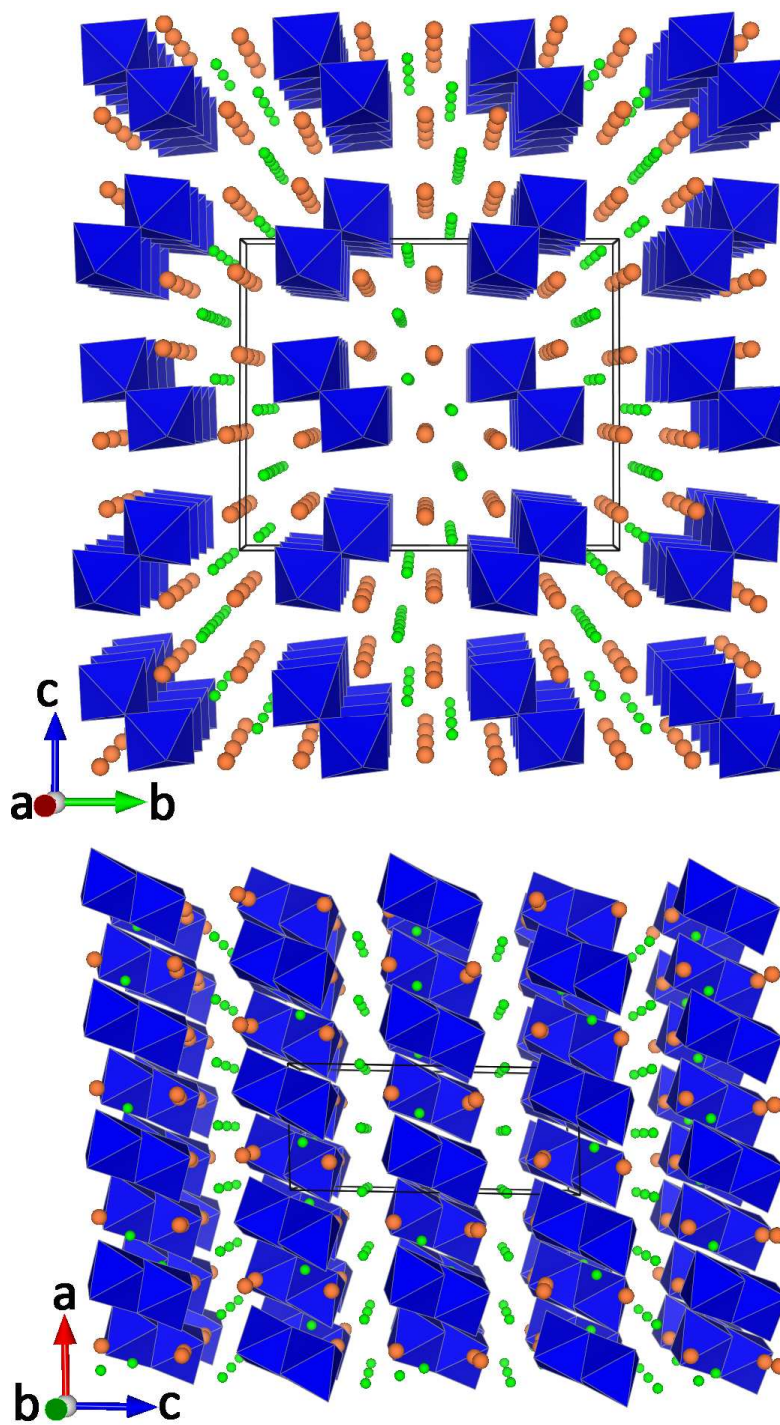
Fig. 6 Polyhedral structure representation of **4**, where the dimeric $V_2O_2F_8$ building blocks are separated by Pb and F atoms. Orange, blue, and green spheres/polyhedra represent Pb, V, and F atoms/polyhedra.
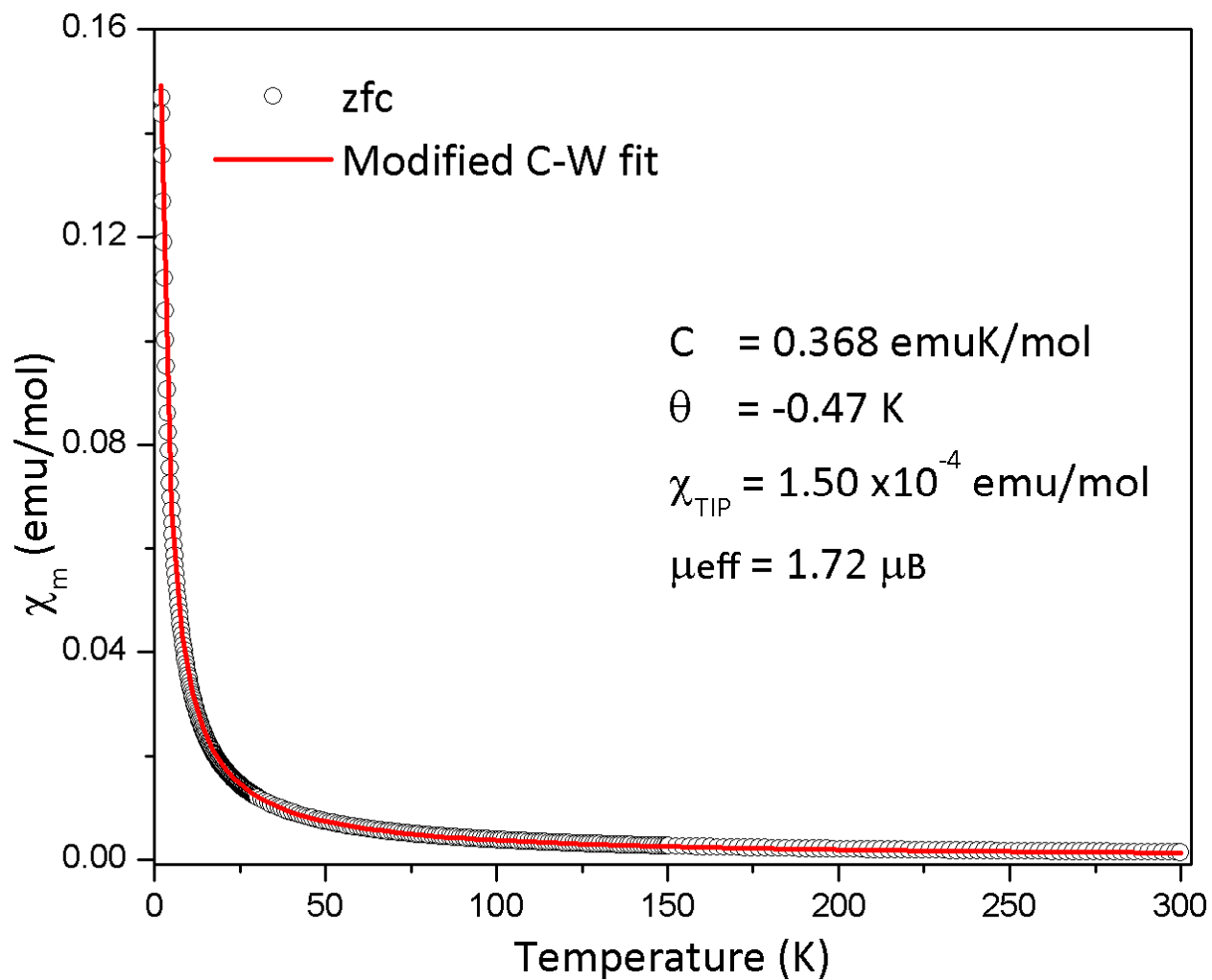
Fig. 7 Temperature dependence of the magnetic susceptibility data for **4** measured under an

applied filed of 1000 Oe, showing paramagnetic behavior. The black circles and red solid line

represent the data and modified Curie-Weiss fit result, respectively.
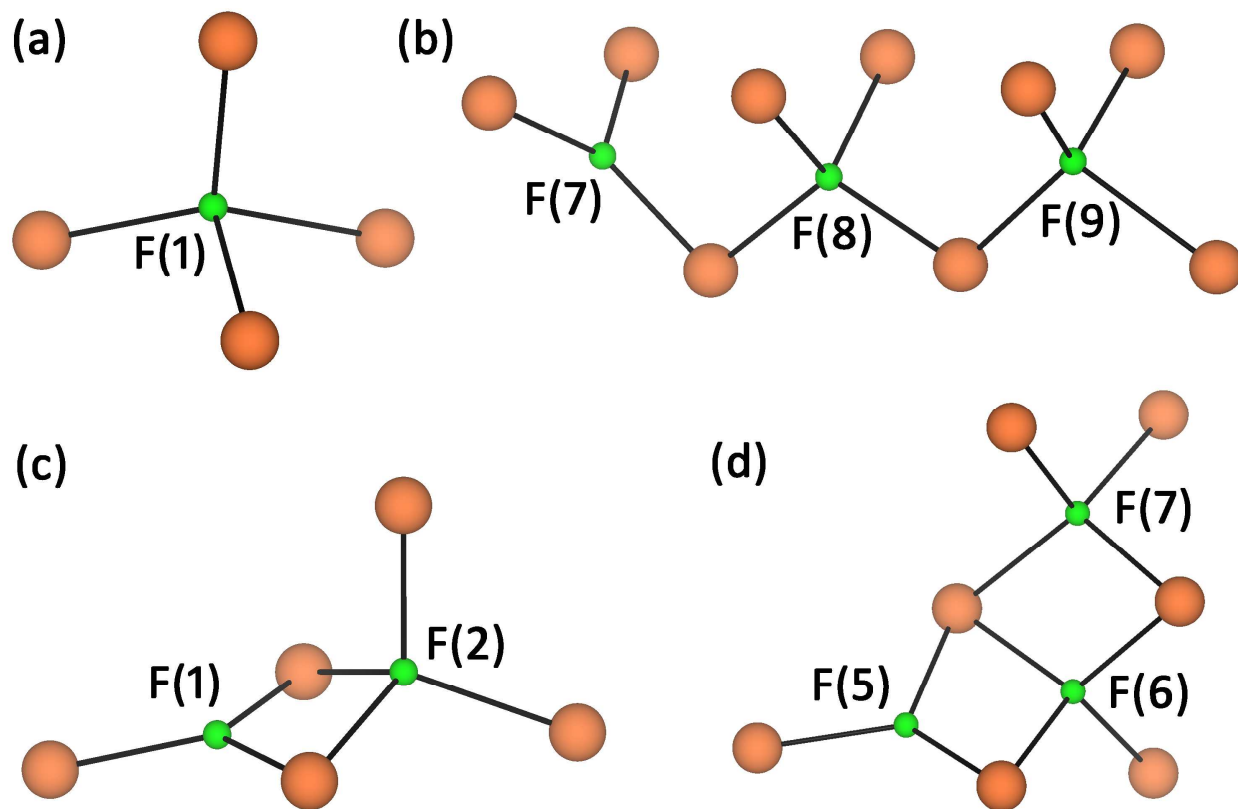
Fig. 8 Ball-and-stick representation of coordination environments for the F_N atoms in (a) **1**, (b) **2**, (c) **3**, and (d) **4** , where the F atoms are found in FA_3 trigonal planar or FA_4 tetrahedra.
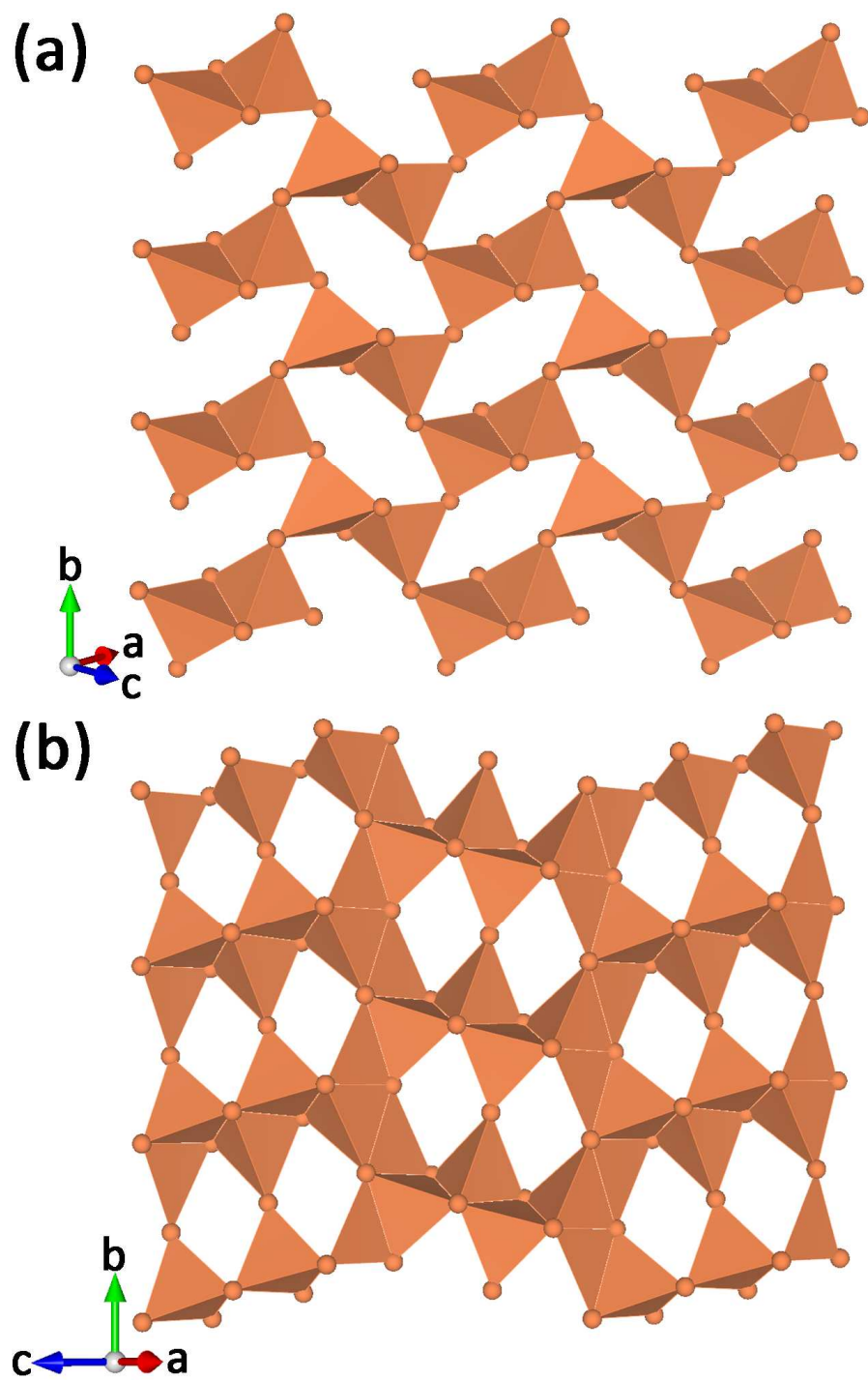
Fig. 9 Illustration of single layers for (a) **1** and (b) **2**, where the corner- or edge-shared $F_N A_3$ or $F_N A_4$ polyhedra create distorted 6- and 4-membered rings in the layers for **1** and **2**, respectively.
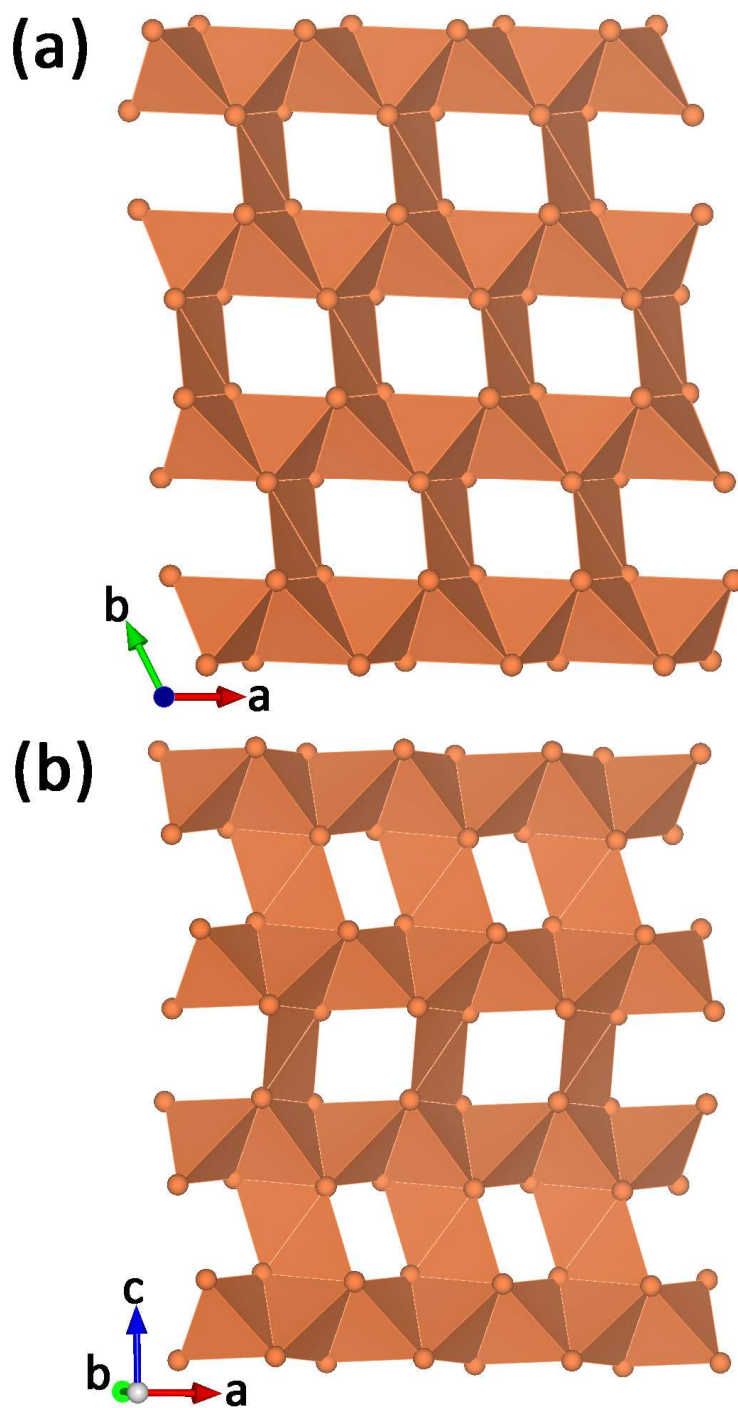
Fig.e 10 Illustration of single sheets for (a) **3** and (b) **4**, where the similar 1-D linear chains composed of edge-edge shared F_NPb_4 tetrahedra and two edge-shared F_NPb_3 trigonal planar connecting the chains are found in both compounds. But, the different arrangement of the edge-shared F_NPb_3 polyhedra results in the distinct formation of the sheets.
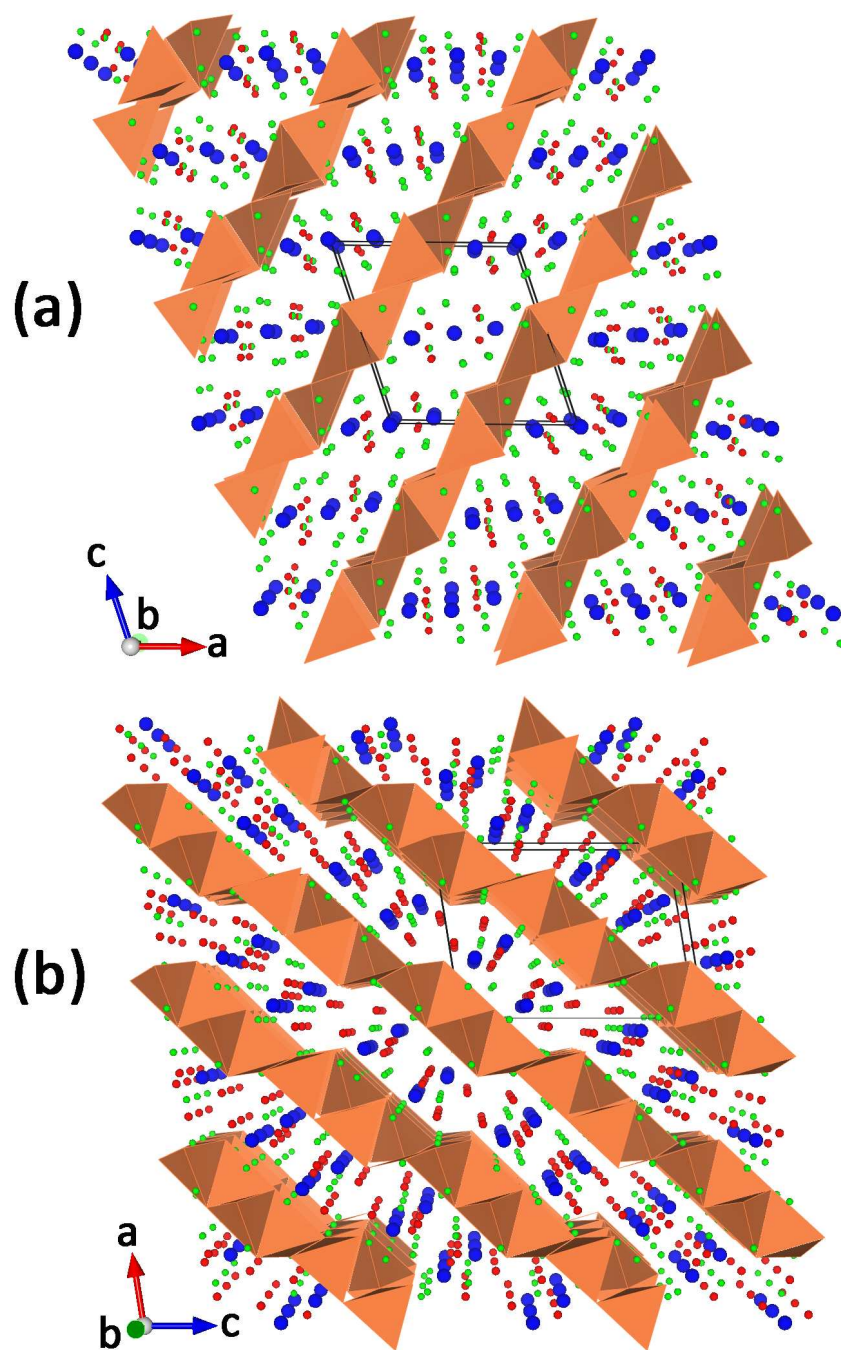
Fig. 11 Illustration of layer stacking manners for (a) **1** and (b) **2**, where the layers separate the VOFs building blocks. For the sake of clarity, the bonds between V and O/F atoms are removed. Orange, blue, red, and green spheres/polyhedra represent F_NPb_x, V, O, and F polyhedra/atoms.
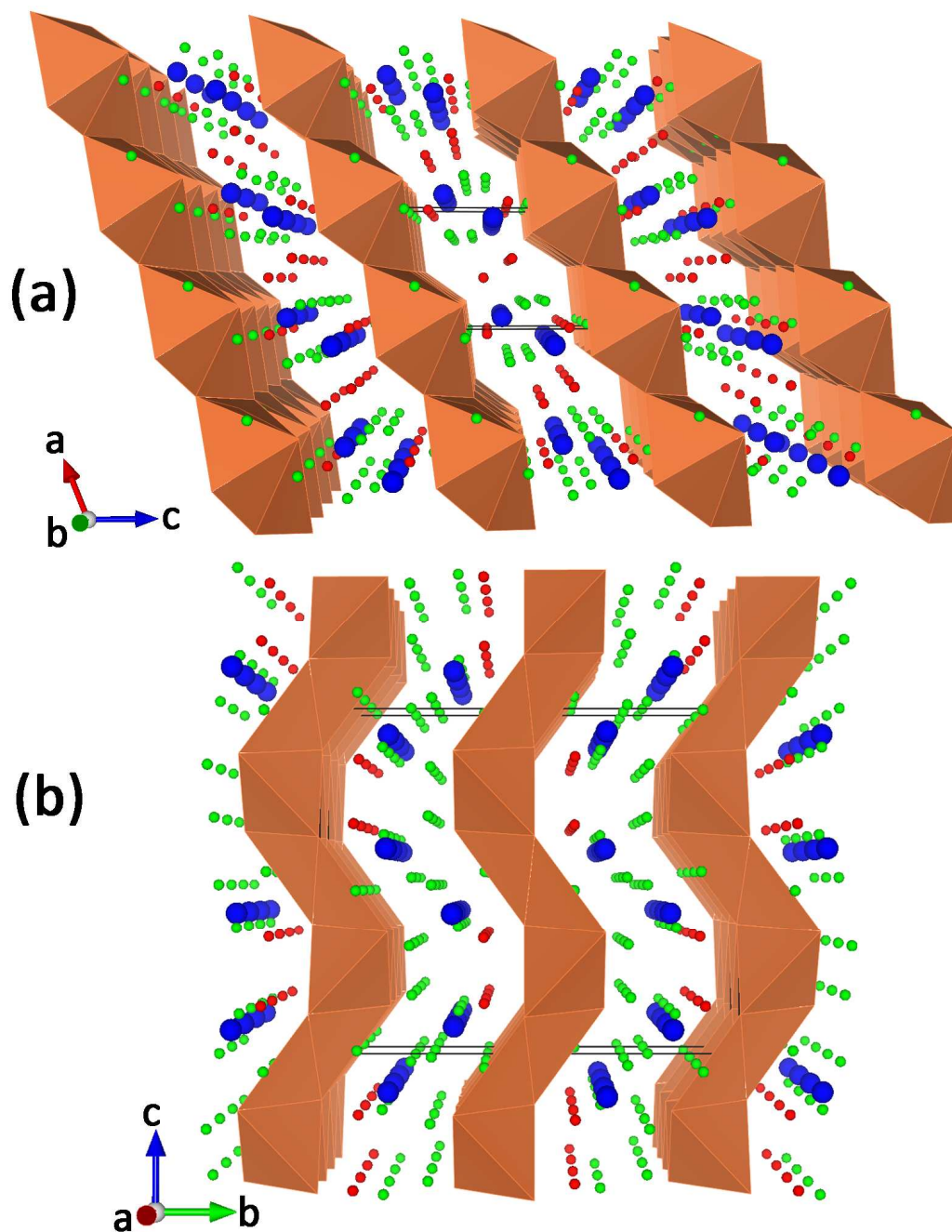
Fig. 12 Illustration of layer stacking fashions for (a) **3** and (b) **4**. Although both compounds exhibit similar dimeric building blocks, different coordination environments around Pb and V atoms result in the distinct layer formation. For the sake of clarity, the bonds between V and O/F atoms are removed. Orange, blue, red, and green spheres/polyhedra represent F_NPb_x, V, O, and F polyhedra/atoms.

Table of Contents

Four novel vanadium oxyfluorides (VOFs) featuring new crystallographic building blocks were crystallized via a mild hydrothermal route.